A New Numerical Method for the problem of Nonlinear Long-Short Wave Interactions

by

Kirki N. Kofiani

MEng., National Technical University of Athens (2007)

Submitted to the Department of Mechanical Engineering
in partial fulfillment of the requirements for the degree of

Master of Science in Ocean Engineering

at the

MASSACHUSETTS INSTITUTE OF TECHNOLOGY

August 2009

Signature of Author ....
Department of Mechanical Engineering
21 August 2009

Certified by ....
Dick K. P. Yue
Philip J. Solondz Professor of Engineering,
Professor of Mechanical and Ocean Engineering
Thesis Supervisor

Accepted by ....
David E. Hardt
Professor of Mechanical Engineering,
Chairman, Committee for Graduate Students

A New Numerical Method for the problem of Nonlinear Long-Short Wave Interactions

by

Kirki N. Kofiani

Submitted to the Department of Mechanical Engineering
on 21 August 2009, in partial fulfillment of the
requirements for the degree of
Master of Science in Ocean Engineering

Abstract

The scope of this thesis is the development of a new numerical method to address the problem of nonlinear interactions of free-surface gravity waves. More specifically, this study addresses the case of wave interactions of short waves ridding on longer waves up to second order of nonlinearity M. The study of the nonlinear interactions between long and short waves is an active research area that has numerous applications.

Most recently the interest on the subject has been regenerated due to the need for reliable prediction of the evolution of large-scale ocean wave-fields using remote sensing techniques for internet-based mapping applications. Accurate deduction of the ocean wave-field elevation requires detailed understanding of the modulation of the wave characteristics due to nonlinear interactions, from both a qualitative and a quantitative perspective.

Initially, we will present the necessary background for the mathematical formulation of the general Nonlinear Wave Interactions (NWI) problem. We will then focus on the High-Order Spectral (HOS) method, a specific mode-coupled method used extensively for the solution of NWI. This method is studied with the objective of developing a new Mapped-Domain Spectral Method (MDSM) that plans to incorporate the strong points of the HOS method and also to extend its capabilities for a broader range of wavelength ratios of NWI.

The new numerical scheme is based on the mapping of the original Boundary Value Problem (BVP) and on the devolopment of a mixed Fourier-Chebyshev spectral method for the solution of the transformed BVP, while ensuring exponential convergence with respect to the Chebyshev order of expansion K.

The investigation of the new method has been conducted for the case of two interacting waves taking into account terms up to $M = 2$. The results agree very well with HOS for cases of wavelength ratios up to $\lambda_S/\lambda_L = 0.1$, as well as for short time evolutions. For cases where either the wavelength ratio is smaller than 0.1, or the run time is significantly larger ($t > 10T_S$), the new method succeeds in providing results, while prior methods are limited by the appearence of divergent terms proportional to $A_L k_S$.

Thesis Supervisor: Dick K. P. Yue
Title: Philip J. Solondz Professor of Engineering,
Professor of Mechanical and Ocean Engineering

Contents

Acknowledgements

I wish to thank my advisor, Professor Dick K. P. Yue for his guidance and encouragement to complete this study and for the advice and help that he provided me with throughout the past two years. I would also like to deeply thank Dr. Yuming Liu for his help and feedback that allowed me overcome several technical difficulties, that I encountered. In addition, I would like to acknowledge and express my gratitude towards Alexander S. Onassis' Public Benefit Foundation for their financial support.

List of Figures

List of Tables

Nomenclature

A	wave amplitude
A_n	amplitude of arbitrary wave mode n
K	maximum Chebychev expansion order
M	perturbation expansion order, nonlinear order
N	number of wave modes, modal resolution
T_k	Chebychev polynomial of order K of the first kind
U_k	Chebychev polynomial of order K of the second kind
V_k	Chebychev polynomial of order K of the third kind
W_k	Chebychev polynomial of order K of the fourth kind
V_g	group velocity
Z	eigenfunction in z- direction
S	eigenfunction in x- direction
a_k, b_k	Fourier coefficients
c_k	coefficient of general orthogonal expansion
f	forcing function in the Poisson equation
g	acceleration of gravity
h	mean depth of Cartesian fluid domain
i	imaginary unit, $i^2 = -1$
k	wavenumber
k_n	wavenumber of arbitrary wave mode n
m	arbitrary perturbation expansion order
n	arbitrary wave mode

p	pressure
u	velocity field in Cartesian domain
t	time variable
x	horizontal spatial coordinate
z	vertical spatial coordinate
Δt	temporal resolution
Δx	spatial resolution
δ	wavelength ratio λ_S / λ_L
ε	wave steepness
η	free-surface elevation
λ	wavelength
ρ	water density
φ	velocity potential in Cartesian domain
φ^S	free-surface velocity potential in Cartesian domain
$\varphi_{(m)}$	velocity potential perturbation expansion term of order m
$\varphi_{m,n}$	velocity potential amplitude of wave mode n and perturbation order m
φ_z	free-surface vertical velocity
ϕ	lower domain velocity potential (Domain II)
ψ_n	eigenfunctions for wave mode n in x- and z- directions

Subscripts

S	denotes short wave variables
L	denotes long wave variables

Superscripts

$\hat{\alpha}$	variable α in mapped domain

Chapter 1

Introduction

In every part of the ocean, there exist different scales of waves that interact producing a complex free-surface. These different scales include, among others, ripples, swells, tidal waves and tsunamis. The long-short wave problem describes the interaction of waves with significantly different wavelengths, like short ripples riding on much longer swells. This problem is of fundamental importance for the understanding of the underlying physics of wave-wave interactions, as well as for a number of engineering applications. More specifically, the nonlinear transfer of energy and momentum consists a crucial part of wave formation and growth. Continuing on this front, we will shortly discuss the significance of Nonlinear Long-Short Wave Interactions (NLSWI) problem for the study of wave growth. Short waves, often called ripples, are initially generated due to the presence of the wind. Their energy is then transported to longer waves through the mechanism of nonlinear wave-wave interactions. This leads to wave growth of longer waves as a result of continuous energy transfer from the wind's side towards the sea surface. Therefore, the solution of the NLSWI problem will help us improve the understanding and modeling of energy transfer and wave growth mechanisms.

The study of the NLSWI is an active research area. Most recently the interest on the subject has been regenerated due to the need for reliable prediction of large-scale wave-fields for web-based applications. Such an application is the real-time adjustment of the routes of travelling vessels to avoid extreme wave events, through accurate wave prediction deduced by Synthetic Aperture Radar (SAR) data. The accurate deduction of the ocean wave-field characteristics requires full understanding of the modulation of the wave characteristics due to general Nonlinear Wave Interactions (NWI). The original goal of this study was the development of a NLSWI capability for extracting information about the long ambient waves, given short wave information, usually provided by remote-sensing techniques.

The path followed in this study starts with an overview of the relevant bibliography for the problem of long-short wave interactions. In order to succeed on that, we investigate the mathematical formulation of the original NWI problem and the numerical implementations used for the solution of this problem in the past. The next step includes focussing on capabilities of methods originally used for NWI, for the solution of the NLSWI problem. The main objective of this step was the assessment of the potential of prior methods for the specific case of NLSWI problem and the identification of extension and improvement areas. The main, highly efficient method used for this purpose was found to be a mode-coupled method called High-Order Spectral (HOS) method, introduced by Dommermuth &Yue in 1987. Therefore, a thorough analysis of HOS has been considered necessary, pinpointing its limitations and proposing a new method that would extend its capabilities for the NLSWI problem. The analytical verification of the effectiveness of a new method has been completed and a new numerical method was developed. The verification of the method for simple cases was conducted. Finally, the case of two interacting waves was addressed for a several values of the study parameters. These parameters were defined to be the wave steepness of the interacting waves, $\varepsilon = Ak$ and the wavelength ratio, $\delta = \lambda_S/\lambda_L$. The analysis of the results as well as the numerical implementation were performed for M up to second order.

Going back to the first step of this analysis, we gathered information about both analytical and numerical results on this problem. In order to accomplish that, a literature survey on the topic of NWI generally and NLSWI in specific was performed in order to collect prior knowledge on both subjects. It has been found that the general area of nonlinear wave interactions of free-surface gravity waves has been extensively investigated in the past by other research groups. More specifically, starting the analysis of prior methods, both Lighthill and Benjamin & Feir worked on the topic focusing their study on side-band instabilities of narrow-band wave-trains (Lighthill 1965, Benjamin & Feir 1967). These results have been succeed by several researchers in the area of nonlinear wave interactions. One of the most important contribution is the derivation of the nonlinear Schrödinger equation for the evolution of a weakly nonlinear narrow-band wave-train using the multiple scale method (Benney & Newell 1967, Chu & Mei 1971, Hasimoto & Ono 1972).

As far as the specific problem of NLSWI is concerned, Longuet-Higgins & Steward used a multiple-scale perturbation method assuming weakly nonlinear waves to provide analytical results for the solution this problem (Longuet-Higgins & Steward 1960). Their results came in a series of papers. The same research group worked also in the evaluation of long-short wave interaction using Stokes' method of approximation as far as second order, assuming unchanged long wave characteristics. They introduced a new term, called radiation stress in the equation of energy in order to justify the modulation of the short waves due to the presence of the long waves. This work was followed by the study of the interactions between short gravity waves while traveling on steady, non-uniform currents considering an asymptotic solution for the velocity potential (Longuet-Higgins & Steward 1960). Bretherton & Garett also produced new results on the topic. They used the conservation of wave action to study the modulation of short waves riding on long waves for the case of very small wavelength ratio λ_S/λ_L (Bretherton & Garett 1968).

In the sequel, there exists the work of Phillips (Phillips 1980) concerning the accurate calculation of the velocity field for a finite-amplitude long wave. The scope of this study was to qualitatively assess the modulation that the short wave suffers, assuming sufficiently small short to long wavelength ratios. In this analysis, the envelop of the short wave amplitude was found to be steady with respect to the surface of the long wave, while the short wave was considered linear.

Proceeding to the strongly nonlinear case, Brueckner, Janda and West worked on the solution of the nonlinear Zakharov free-surface boundary condition using the Watson-West Method (WWM) for the case of strongly nonlinear long-short wave interaction. They considered the case of short-long wavelength ratio equal to $k_S/k_L = 1/8$ (Brueckner, Janda, West 1986). This study included both resonant and non-resonant cases of wave interactions and leaded to the following physical outcomes. a) Non-steady maximum modulation of the short wave while travelling on the long wave. b) The maximum modulation is not necessarily located in the crest of the long wave. c) Lock-in phenomena prevent the short waves from traveling freely onto the long waves.

Phillips also continued his work in this area, studying the effects of energy transfer from the wind to short waves and of energy loss due to existence of wave breaking (Phillips 1984). He also investigated the range of validity of wave-wave interactions that can be address in the case where both the long and short waves are considered weakly nonlinear. About the same time, a new methodology was proposed by Zhang to study the modulation of a short wave riding on a long wave. This method was based on orthogonal curvilinear coordinates (Zhang 1987).

After following the path of former researchers in the field of nonlinear wave interactions and nonlinear long-short wave interactions, an extensive investigation was performed in order to identify possible contribution areas. Finally, the need of an effective numerical methodology that would address the fully nonlinear case of NLSWI was identified. Past researchers analytically calculated the modulations of both the amplitude and the wavelength of the short wave up to only third order of nonlinearity. Analytical attempts were abandoned since higher order calculations are analytically intractable. Proceeding to the study of numerical methods employed for the solution of the NLSWI problem, Mode-Coupling Methods (MCM) were introduced for the general nonlinear wave-wave interactions accounting up to an arbitrary nonlinear order M of N interacting waves (Dommermuth & Yue 1987). However, a systematic study of NLSWI using MCM has not yet been conducted, according to our knowledge. This is the starting point of this study. After extensive analysis, the need for developing a robust, direct numerical method for NLSWI was identified as the contribution area of this thesis. Because of the complexity of the problem, this thesis targeted the solution of the NLSWI problem up to second order of nonlinearity M following the path of prior researchers (Longuet.Higgins & Steward 1960).

In order to reach this goal we had to move a step back again and study the general NWI problem. This problem has been solved in the past for up to a specific range of wavelength ratios. The main numerical method used for that reason was the HOS method. This powerful numerical technique uses a perturbation expansion of the field variables in terms of a small parameter ε, that is a measure of typical wave steepness. Then, a Taylor expansion about the mean free-surface, $z = 0$, is employed for the calculation of the free-surface variables in terms of the mean free-surface variables. The process is completed with the formulation and numerical integration of the evolution equations in order to proceed to the next time step. The problem is described and solved sequentially for each perturbation order M and the results are summed up to an arbitrary order defined in advance, for each time step t. The use of the Taylor expansion about the mean free-surface has been studied systematically in the HOS formulation. The conclusion of this study was that the use of the Taylor expansion was responsible for the limited range of wavelength ratio validity of HOS. In order to overcome this restriction, we developed a new numerical method, called Mapped-Domain Spectral Method (MDSM). The new method follows the idea of HOS, expanding the field variables in terms of a small parameter ε. However, the analytical basis of this method lies on a mathematical transformation of the original coordinate system into an equivalent one that will allow for the formulation and solution of an equivalent boundary value problem without using the Taylor expansion about the mean free-surface. This trasformation was originally introduced for the solution of optics problems (Nicholls & Reitich 2004 a, b).

The first step of the development of this new method lies in the identification of an appropriate coordinate transformation that will allow us to overcome the problems introduced by the Taylor expansion. This appropriate transformation was located and by applying it, the geometry of the original fluid domain changed from an unsteady free-surface domain, into a steady, rectangular domain. In this new domain the Taylor expansion about $z = 0$ is no longer necessary. However, the mapping also changed the expression of the field equations. Originally, the field equation was a Laplace's equation, which was turned into a Poisson equation after the performed transformation. In order to solve the problem in the mapped domain, we developed a new spectral numerical scheme. After locating the most appropriate transformation and solving the mapped boundary value problem, we needed to proceed to the calculation of the free-surface vertical velocity in the original domain. In order to do that we use the inverse mapping and calculate the vertical velocity with respect to the mapped domain variables. The cycle closed by substituting the vertical velocity in the evolution equation and calculating the free-surface elevation and velocity potential for the next time step using the HOS, fourth order Runge-Kutta integration in time.

The solution of the NLSWI problem, in five consecutive steps is given below:

- Mathematical formulation of the Boundary Value Problem (BVP) in classical Cartesian coordinates

- Analysis and reformulation of the original BVP in an appropriately chosen mapped domain
- Development of an efficient spectral solver of the new, mapped BVP
- Transformation between the physical and mapped domain of information for the calculation of the free-surface vertical velocity in Cartesian coordinates
- Time integration for the evaluation of the free-surface time history using former HOS time evolution scheme

This thesis is organized in Chapters as follows. In the second Chapter the mathematical formulation of the general problem of nonlinear wave interactions is presented and the Zakharov formulation used for the derivation of the evolution equation of the problem of NWI is introduced. The third Chapter deals with the investigation of the specific mode coupling method, the HOS method. The capabilities and limitations of this method for the solution of the NWI problem are studied. The method is tested for the case of two interacting waves, a long and a short wave. In the fourth Chapter, the problem of NWI is revisited and reformulated accordingly to treat cases of wavelength ratios that could not be addressed effectively in the past. A new mathematical formulation is proposed for these specific cases and the analytical investigation of the method is illustrated. In Chapter 5, the numerical implemerical of the formulation proposed in Chapter 4 is demonstrated in a number of steps. Each step is evaluated seperately and results are shown to support that each step was solved in an optimum manner. Finally, the new method, MDSM for the solution of the problem of NLSWI is introduced and assessed for the case of two interacting waves for M up to second order. The thesis concludes in Chapter 6, with a discussion over the numerical results of MDSM and ideas for future work. The four appendices serve as supplementary material that was necessary for the analysis of the thesis but could not be included in the body of the Chapters to avoid discursiveness.

Chapter 2

General Problem of Nonlinear Wave Interactions (NWI)

2.1 Mathematical Formulation

We start our analysis with the mathematical formulation of nonlinear water wave motion. This problem is treated under the assumptions of 2D, irrotational motion of a homogeneous, incompressible and inviscid fluid. The free-surface is denoted by $\eta(x,t)$ and the fluid domain has an arbitrary depth h (Fig. ??). The above mentioned assumption leads to the formulation of a potential flow problem. More specifically, the velocity field is given by the following expression

$$u(x,z,t) = \nabla\varphi(x,z,t)\,, \tag{2.1}$$

where $u(x,z,t)$ is the velocity field and $\varphi(x,z,t)$ represents the velocity potential.

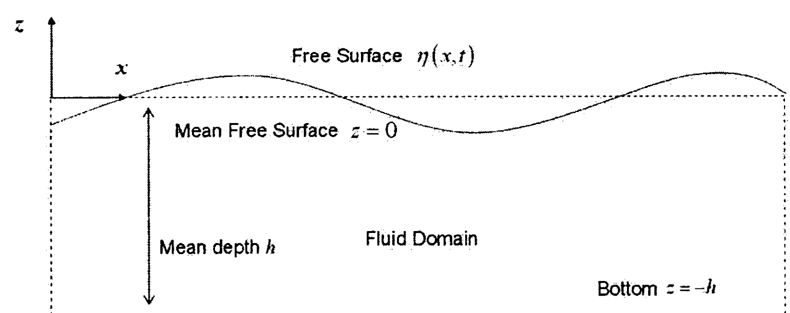

Figure 2-1: Problem configuration of NWI problem in Cartesian coordinates

The governing equations of the problem are given by the continuity equation for the velocity field and the Bernoulli equation for the pressure distribution inside the fluid domain. The continuity equation under the above mentioned assumptions is given by the Laplace equation,

$$\nabla^2 \varphi (x, z, t) = 0. \tag{2.2}$$

This equation is solved independently from Bernoulli's equation to obtain the velocity potential $\varphi (x, z, t)$. Then, the velocity potential is substituted in the Bernoulli equation to calculate the pressure within the fluid domain. Laplace's equation is accompanied by the boundary conditions on the free-surface, $z = \eta$ and bottom, $z = h$. On the free-surface, the boundary conditions are described below.

a) The kinematic boundary condition is given by the expression

$$\frac{\partial \eta}{\partial t} + \frac{\partial \varphi}{\partial x} \cdot \frac{\partial \eta}{\partial x} - \frac{\partial \varphi}{\partial z} = 0. \tag{2.3}$$

This expression is based on the argument that the free-surface $\eta (x, t)$ is a material surface. In order to derive the above expression we take the material derivative of the description of the free-surface,

$$z - \eta (x, t) = 0.$$

The fact that the free-surface is a material surface is described by

$$\frac{D}{Dt} (z - \eta (x, t)) = 0.$$

This leads to

$$\frac{\partial}{\partial t} (z - \eta (x, t)) + u \cdot \nabla (z - \eta (x, t)) = 0$$

$$\frac{\partial (z - \eta (x, t))}{\partial t} + (u, w) \left(\frac{\partial (z - \eta (x, t))}{\partial x}, \frac{\partial (z - \eta (x, t))}{\partial z} \right) = 0$$

$$\frac{\partial \eta}{\partial t}+\left(\frac{\partial \varphi}{\partial x}, \frac{\partial \varphi}{\partial z}\right)\left(\frac{\partial\left(z-\eta\left(x,t\right)\right)}{\partial x}, \frac{\partial\left(z-\eta\left(x,t\right)\right)}{\partial z}\right)=0$$

$$\frac{\partial \eta}{\partial t}+\left(\frac{\partial \varphi}{\partial x}, \frac{\partial \varphi}{\partial z}\right)\left(\frac{\partial \eta}{\partial x},-1\right)=0$$

Therefore the kinematic boundary conditions is given by

$$\frac{\partial \eta}{\partial t}+\frac{\partial \varphi}{\partial x} \cdot \frac{\partial \eta}{\partial x}-\frac{\partial \varphi}{\partial z}=0.$$

b) The dynamic boundary condition is expressed accordingly by the Bernoulli's law

$$\frac{\partial \varphi}{\partial t}+\frac{1}{2} \cdot|\nabla \varphi|^2+g z+\frac{p}{\rho}=0.$$

This expression represents the equilibrium of forces at the free-surface $z=\eta\left(x,t\right)$. The pressure on the free-surface is taken to be zero and therefore the dynamic boundary condition on the free-surface is given by

$$\frac{\partial \varphi}{\partial t}+\frac{1}{2} \cdot|\nabla \varphi|^2+g \eta=0. \tag{2.4}$$

After the previous section analysis, we will proceed to the description of the governing equations and boundary conditions for the velocity potential φ. In the following analysis, we will not deal with the pressure distribution within the fluid domain.

2.2 Governing Equations of NWI

Based on the analysis of the previous paragraph, we can now proceed to the full description of the governing equation of the nonlinear interaction problem. The equation for the velocity potential φ is given by

$$\nabla^2 \varphi(x, z, t)=0, \qquad \text{where } (x, z) \in[0,2 \pi] \times[-h, \eta(x, t)], \tag{2.5}$$

where $\eta\left(x,t\right)$ is the free-surface elevation, $\varphi(x, z, t)$ the velocity potential and h is the mean depth of the fluid domain. The governing equation is accompanied by the associate free-surface boundary conditions, that is as mentioned earlier, the kinematic condition

$$\frac{\partial \eta}{\partial t} + \frac{\partial \eta}{\partial x} \cdot \frac{\partial \varphi}{\partial x} - \frac{\partial \varphi}{\partial z} = 0 \tag{2.6}$$

and the dynamic condition, both at $z = \eta(x,t)$

$$\frac{\partial \varphi}{\partial t} + \frac{1}{2} \cdot |\nabla \varphi|^2 + gz = 0. \tag{2.7}$$

Finally, we have the bottom boundary condition, at $z = -h$, that is different according to whether we consider deep water of finite depth. More details for the bottom boundary conditions will be given in later chapters.

2.3 Zakharov's mode coupling model

In order to solve the above problem, several approaches have been used in the past. Most of those methods solved the problem as it was described in Section 2.2. However, in 1968, Zakharov introduced a new variable for the description of this problem. This variable was the free-surface velocity potential, denoted by φ^S. The original free-surface boundary conditions were then reformulated with respect to φ^S and a new evolution equation was presented. In this study, we shall follow Zakharov's mode coupling idea (Zakharov 1968). We initially introduce, same as Zakharov did, the free-surface velocity potential φ^S that is defined by the following expression

$$\varphi^S(x,t) = \varphi(x, \eta(x,t), t). \tag{2.8}$$

The free-surface boundary conditions is then transformed in terms of the free-surface velocity potential φ^S. The detailed process of the reformulation is presented in the relevant literature. We will only present the basic ideas of the method. One of the main ideas is the fact that the time and space derivatives of φ^S are calculated using the chain rule with respect to $\eta(x,t)$. More specifically, the time derivative of the free-surface velocity potential is given by

$$\frac{\partial}{\partial t}\varphi^S(x,t) = \frac{\partial \varphi}{\partial t} - \frac{\partial \varphi^S}{\partial z} \cdot \frac{\partial \eta}{\partial t} \tag{2.9}$$

and the x-space derivative is accordingly

$$\frac{\partial}{\partial x}\varphi^S(x,t) = \frac{\partial \varphi}{\partial x} - \frac{\partial \varphi^S}{\partial z} \cdot \frac{\partial \eta}{\partial x}. \tag{2.10}$$

The free-surface velocity potential is not a function of the vertical coodinate as it is demonstrated in Eq. (2.8). The free-surface kinematic boundary conditions at $z = \eta(x,t)$, is then transformed in terms of φ^S accordingly

$$\frac{\partial \eta}{\partial t} + \frac{\partial \varphi^S}{\partial x} \cdot \frac{\partial \eta}{\partial x} - \left(1 + \left(\frac{\partial \eta}{\partial x}\right)^2\right)\frac{\partial \varphi}{\partial z} = 0. \tag{2.11}$$

The dynamic condition at $z = \eta(x,t)$ is similarly trasformed

$$\frac{\partial \varphi^S}{\partial t} + \frac{1}{2} \cdot \left(\frac{\partial \varphi^S}{\partial x}\right)^2 + g\eta - \frac{1}{2} \cdot \left(1 + \left(\frac{\partial \eta}{\partial x}\right)^2\right) \cdot \left(\frac{\partial \varphi}{\partial z}\right)^2 = 0. \tag{2.12}$$

The above equations are called evolution equation and are used to solve for φ^S and η, for every time step. These equations are driving the dynamics of the free-surface elevation and velocity potential.

2.4 Perturbation Expansion

For the scope of our analysis, we assume that the free-surface η is of order ε, where ε is the representative steepness. We expand also assume that the velocity potential can be expand in terms of ε up to a certain given order M

$$\varphi(x,z,t) = \sum_{m=1}^{M} \varphi_{(m)}(x,z,t). \tag{2.13}$$

Each order $\varphi_{(m)}$ contains N free waves, namely

$$\varphi_{(m)}(x,z,t) = \sum_{n=1}^{N} \varphi_{m,n}(t)\,\psi_n(x,z), \tag{2.14}$$

where $\psi_n(x,z)$ are the eigenfunctions of the problem in the $x-$ and $z-$directions. By assumption, we use periodic boundary conditions in the $x-$ direction. Therefore, as far as the dependence in the $x-$direction, we have that

$$\psi_n(x,z) = Z(z) \cdot \exp(ik_n x) \tag{2.15}$$

As far as the $z-$ direction is concerned, the expression of ψ_n depends on the bottom boundary conditions. a) For deep-water regime problems, the bottom boundary condition requires that $\nabla\varphi \to 0$ at $z \to \infty$.This leads to $Z(z) = \exp(k_n z)$. Therefore, the expression for the eigenfunctions is given by

$$\psi_n(x,z) = \exp(k_n z + ik_n x). \tag{2.16}$$

b) For finite-water depth regime problems on the other hand, the expression of the bottom boundary condition becomes, $\frac{\partial\varphi}{\partial z} = 0$ at $z = -h$. This leads to the following expression for the $z-$ dependence, $Z(z) = \cosh(k_n(z+h))$. Therefore, we have that

$$\psi_n(x,z) = \cosh(k_n(z+h)) \cdot \exp(ik_n x). \tag{2.17}$$

As it was mentioned earlier, we assume that the free-surface is of order ε and that the velocity potential is given by Eq. (2.13). According to these assumptions, we can formulate the problem in orders and gather the results up to an arbitrary order M. We will now proceed to the description of the first, i.e $M = 1$ The first order problem governing equation is therefore given by

$$\nabla^2\varphi_{(1)}(x,z,t) = 0, \qquad \text{where } (x,z) \in [0,2\pi] \times [-h, \eta(x,t)] \tag{2.18}$$

with the associated kinematic

$$\frac{\partial\eta}{\partial t} - \frac{\partial\varphi_{(1)}}{\partial z} = 0 \tag{2.19}$$

and dynamic boundary condition at $z = 0$,

$$\frac{\partial\varphi^S_{(1)}}{\partial t} + g\eta = 0. \tag{2.20}$$

Every order problem is solved sequential up to a given order M. The second and higher order problems are described in the relative literature. This methodology can solve the general nonlinear interaction problem for up to an arbitrary nonlinear order M accounting for a given number of interacting waves N. The numerical implementation of the problem will be presented in the next chapter for up to an arbitrary order M. Two research groups have worked independently on this aspect and their work has been presented in two separate papers, Dommermuth&Yue (1987) and West, Brueckner & Janda (1987). Following this literature, we will proceed to the presentation of the method Both methods follow similar paths. However, throughout this thesis we will use the nomenclature and terminology of the former research group.

Chapter 3

High Order Spectral Method (HOS)

3.1 Numerical formulation of NWI

The high order spectral method was introduced on the same year by Dommermuth&Yue and West, Brueckner & Janda in 1987. Following the assumptions of 2D, irrotational motion of an homogeneous, incompressible and inviscid fluid, the velocity field of the flow is fully described by the velocity potential $\varphi(x, z, t)$. With in the fluid domain the velocity potential satisfies Laplace's equation as a consequence of the continuity equation. We assume that the free-surface is of order ε and the velocity potential can be represented by a perturbation series in ε

$$\varphi(x, z, t) = \sum_{m=1}^{M} \varphi_{(m)}(x, z, t), \tag{3.1}$$

where $\varepsilon = kA$ represents the free-surface steepness where k and A the relevant wavenumber and wave amplitude or the problem of interest. We expand each term of the perturbation series for the expression of the velocity potential φ about the mean free-surface, $z = 0$, as shown below, in order to describe the free-surface variables in terms of mean-free surface quantities

$$\varphi^S(x, t) = \varphi(x, z = \eta(x, t), t) = \sum_{m=1}^{M} \sum_{k=0}^{M-m} \frac{\eta^k}{k!} \frac{\partial^k}{\partial z^k} \varphi_{(m)}(x, 0, t). \tag{3.2}$$

Given the above description, we formulate a series of boundary value problems that are to be solved sequentially, starting from $M = 1$

$$\begin{aligned} R^{(1)} &= \varphi^{S}(x,t) \\ &\vdots \\ R^{(m)} &= \sum_{k=0}^{M-1} \frac{\eta^{k}}{k!} \frac{\partial^{k}}{\partial z^{k}} \varphi_{(m-k)}(x,0,t) \end{aligned} \tag{3.3}$$

Each order of the velocity potential $\varphi_{(m)}$ contains N free-waves. Because of that, every order is expanded in terms of eigenfunctions ψ_n,

$$\varphi_{(m)}(x,z,t) = \sum_{n=1}^{N} \varphi_{m,n}(t)\,\psi_n(x,z). \tag{3.4}$$

The next crucial step is the calculation of the free-surface vertical velocity φ_z for every order

$$\frac{\partial \varphi_{(m)}}{\partial z}(x, z = \eta(x,t), t) = \sum_{k=0}^{M-m} \frac{\eta^{k}}{k!} \frac{\partial^{k+1}}{\partial z^{k+1}} \sum_{n=1}^{N} \varphi_{m,n}(t)\,\psi_n(x,0). \tag{3.5}$$

The total free-surface vertical velocity is the sum of $\frac{\partial \varphi_{(m)}}{\partial z}$ for $m = 1, ..., M$.

$$\varphi_z = \sum_{m=1}^{M} \sum_{k=0}^{M-m} \frac{\eta^{k}}{k!} \frac{\partial^{k+1}}{\partial z^{k+1}} \sum_{n=1}^{N} \varphi_{m,n}(t)\,\psi_n(x,0) \qquad \text{at } z = \eta(x,t). \tag{3.6}$$

The expression of φ_z is then substituted in the Zakharov reformulated free-surface kinematic and dynamic boundary conditions that is expressed in terms of φ^S. These equations are called the evolution equations of the problem and are described in terms of the modal amplitudes $\varphi_{m,n}$. Given that, we can obtain the free-surface elevation and the free-surface velocity potential for the next time step. This procedure repeats to obtain, the phase resolved time history of the free-surface elevation for the initial wave field. This methodology has been numerically implemented to cover the 3D case (SNOW) and include wave-current, wave-wind and wave-bottom interactions as well as wave-breaking dissipation effects.

3.2 Capabilities of HOS for solving the general NWI problem

HOS is a powerful nonlinear mode-coupling, pseudo-spectral method used for the modeling of irrotational free-surface gravity waves. This method has many capabilities. More specifically, the strengths of this method are:

- Accounts for up to an arbitrary order M of nonlinear interactions with up to $O(N)$ modal resolution of free-waves
- The computational effort is proportional to $O(M\ N\ logN)$
- Able to treat both the 2D and the 3D case of nonlinear gravity waves
- HPC scalable
- Used to model wave-wave, wave-current as well as wave-body interactions
- Spacial resolution of the order $O(km)$ wave field forecast (SNOW)

3.3 Limitations of HOS for solving the NLSWI problem

Although, HOS is a powerful method there are some limitations which need to be discussed.

General issues encountered:

- The first point that needs attentions is the CFL condition. To be more specific, the Courant-Friedrich-Lewy condition is given by $V_g \cdot \Delta t < \Delta x$, where $V_g = \frac{1}{2}\sqrt{\frac{g}{k}}$ is the deep water group velocity, Δt the temporal resolution and Δx the spacial resolution. If the CFL condition is not satisfied, then we cannot calculate the time history of the free-surface elevation and velocity potential. It is important to note that for all cases that we need to study, we must always verify that the results are independent of the time and space resolutions. For that reason, we compared results obtained for a number of different values of Δt, for given Δx and initial conditions. In order to trust the results they need to be independent from Δt, Δx provided that the CFL condition is satisfied.

- Another delicate point was related to the application of the initial conditions in HOS. The computational space domain for which we calculated the initial conditions need to be $[0, 2\pi)$. If for any case we used a different domain, e.g. $[0, 2\pi]$, the results deteriorated in only few time steps. More specifically, the deterioration initiates near the ends of the domain in the form of high frequencies as it is shown in Fig.(3-1). These frequencies amplified fast causing the rest of the solution to fail. This issue was completely resolved after using the closed-open domain, $[0, 2\pi)$ for the calculation of the initial conditions.

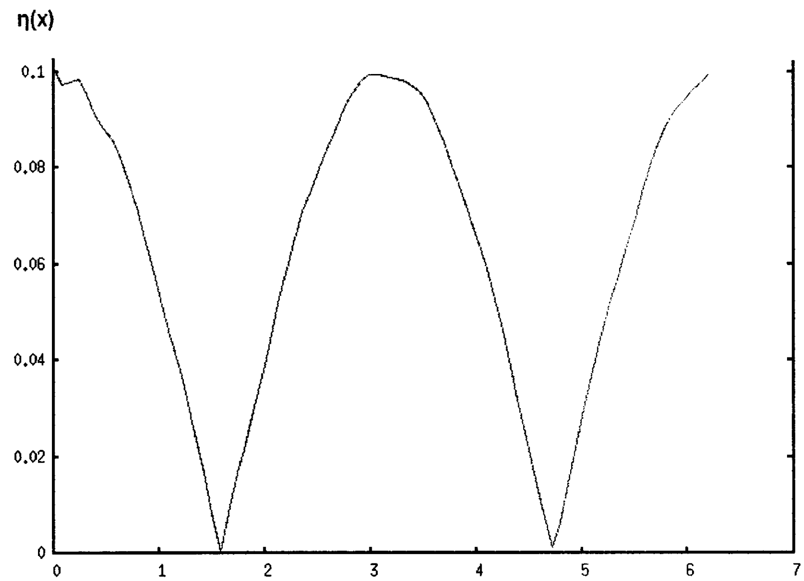

Figure 3-1: Absolute value of the free-surface elevation at a specific time step $t = t_N$

- The last important issue that we faced, while using HOS, was related to the wave steepness ε. For cases where ε exceeded the value of 0.35 the simple HOS version used for our analysis deteriorated. The cause of this problem lies in the description of the problem. The use of a perturbation expansion is limited by the value of the steepness. If $\varepsilon > \varepsilon_{\max}$, then the formulation for φ_z is no longer valid. This is a general limitation of the family of mode-coupling methods that lies on the validity of the perturbation expansion, which is introduced by the steepness ε of the wave-modes. This problem however was treated and incorporated in a new HOS version by the introducing a filter to simulate wave breaking effects.

The above mentioned problems affect the general treatment of the problem for the prediction of phase-resolved wave evolution. They were appropriately treated nowadays and for that reason we will not spend any more time studying them, since they do not interfere directly with the problem of nonlinear long-short wave interactions. However, there was an extra problem that emerged while investigating HOS. This issue was specifically affecting the problem of NLSWI. It involved the dependence of the results on the computational precision used for the calculations. As the computer accuracy was increased better results were produced and simulations run for longer times. This problem was found to originate from the use of Taylor expansion about the mean free-surface due to the appearence of divergent terms proportional to $A_L k_S$. In order to demonstrate the above point, we will present the results from the case investigation of $\delta = \lambda_S/\lambda_L = 0.1$ and $\varepsilon = kA = 0.1$. The results from this case show the comparison between η and φ at the initial step $t = 0$ and at $t = 41$ ts (time steps). We can see clearly the introduction of non-physical frequencies in the solution. The numerical solution stopped in the next time step because the vertical velocity could not be evaluated. The interesting result was that for a given initial condition and nonlinear order M, the time step of divergence was found to depend on the computational accuracy. On the same spirit, for given initial conditions and total number of time steps, the divergent nonlinear order M was found to be dependent also on the computional accuracy.

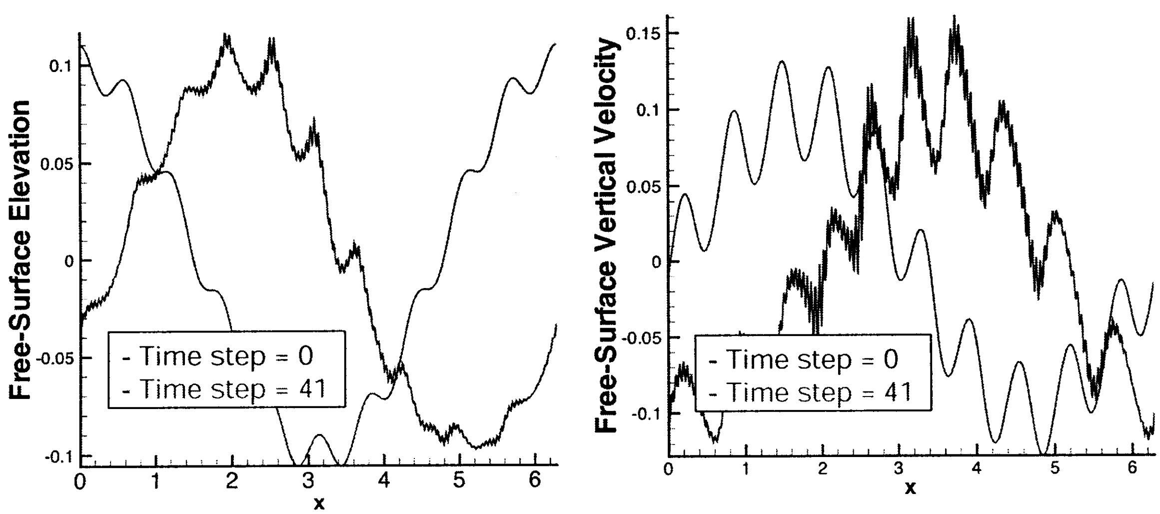

Figure 3-2: Simulation of NLSWI for $\delta = 0.1$ and $\varepsilon = 0.1$ and 16 digits computational precision. Comparison of η and φ^S at $t = 0$ and $t = 41$ ts.

By increasing the computational precision, we managed to extend the run time of the simulation and also obtain results for higher order of nonlinearity. The following table demonstrates for the above case, how the computational accuracy affected both the run time (in terms of time steps) and the nonlinear order.

Computational Precision	Divergence parameters	
	M	Time Step
8	4	27
16	5	41

Table 3-1: Computational accuracy vs. divergence parameters

This is a more interesting topic and it affects the effectiveness of the method regarding the treatment of the NLSWI. This limitation of HOS stems, as it was mentioned earlier from the use of the Taylor expansion about the mean free-surface, $z = 0$. In the next section we will further investigate this problem.

3.4 Appearence of divengent terms

The use of the Taylor expansion causes the appearance of divergent terms in the expression of the free-surface vertical velocity when calculated in terms of the initial conditions at the free-surface. More specifically, we will investigate the case of two wave-modes,$N = 2$, a long and a short one, with wave characteristics A_L, k_L and A_S, k_S. The velocity potential $\varphi(x, z, t)$ is expressed as a perturbation expansion of $\varepsilon = A_L k_L = A_S k_S$, which represents the relevant wave steepness of the problem. For our analysis, we assume that the two waves have the same steepness. The velocity potential is given by

$$\varphi(x, z, t) = \sum_{m=1}^{M} \varphi_{(m)}(x, z, t). \tag{3.7}$$

Each order $\varphi_{(m)}$ contains N wave modes. Given the free-surface velocity potential φ^S and the free-surface elevation η at $t = 0$, in the case of deep water, we formulate the boundary value problem for $\varphi_{(m)}$ for every order m.

$$\varphi_{(m)}(x,z,t) = \sum_{n=1}^{N=2} \varphi_{m,n}(t)\, e^{k_n z} \varphi_n(x,t)\,, \tag{3.8}$$

for each order

$$\begin{aligned} \varphi_{(m)}(x,0,t) &= R^{(m)}, \text{ where} \\ R^{(1)} &= \varphi^S(x,t) \\ R^{(2)} &= -\eta \frac{\partial}{\partial z} \varphi_{(1)}(x,0,t) \\ &\vdots \\ R^{(m)} &= -\sum_{k=1}^{m-1} \frac{\eta^k}{k!} \frac{\partial^k}{\partial z^k} \varphi_{(m-k)}(x,0,t)\,. \end{aligned} \tag{3.9}$$

The expression of the free-surface vertical velocity is given by

$$\varphi_z(x, z=\eta(x,t), t) = \sum_{m=1}^{M} \sum_{k=0}^{M-m} \frac{(\eta)^k}{k!} \sum_{n=1}^{N=2} \varphi_{m-k,n}(t) \frac{\partial^k}{\partial z^k} \varphi_n(x,0) \tag{3.10}$$

We assume that the free-surface consists of two linear waves, $\eta(x,t) = A_L \sin(k_L \cdot x) + A_S \sin(k_S \cdot x)$ at $t=0$. This leads to the appearance of terms proportional to $A_L \cdot k_S = O(1)$ as it is shown below

$$\begin{aligned} A_L k_L &= O(\varepsilon)\,, \\ A_S k_S &= O(\varepsilon)\,, \\ \frac{k_L}{k_S} &= O(\varepsilon)\,. \end{aligned}$$

$$A_L k_S = O(\varepsilon) \frac{k_S}{k_L} = O(1)$$

This result suggests that in the description of the vertical velocity we have the appearence of $O(1)$ terms, $A_L k_S$. Therefore, we expect that the numerical scheme should diverges for every similar case. However, the use of mode-coupled methods for the solution of NWI was vindicated by Brueckner &West in 1988. The divergent terms were found to cancelanalytically for each nonlinear order M. We can show this for the simple case of two interacting wave modes, and up to third order of nonlinearity considered, $M = 3$. In this case the expression of the free-surface vertical velocity φ_z is given by

$$\begin{aligned} \varphi_z &= \varphi_L^S \cdot k_L \left(1 + \frac{\eta \cdot k_L}{1!} + \frac{\eta^2 \cdot k_L^2}{2!} - \frac{\eta \cdot k_L}{1!} - \frac{\eta \cdot k_L^2}{1!} + \frac{\eta^2 \cdot k_L^2}{2!}\right) \sin\left(k_L \cdot x\right) + \\ &+ \varphi_S^S \cdot k_S \left(1 + \frac{\eta \cdot k_S}{1!} + \frac{\eta^2 \cdot k_S^2}{2!} - \frac{\eta \cdot k_S}{1!} - \frac{\eta \cdot k_S^2}{1!} + \frac{\eta^2 \cdot k_S^2}{2!}\right) \sin\left(k_S \cdot x\right) \end{aligned}$$

where $\eta(x,t) = A_L \sin(k_L \cdot x) + A_S \sin(k_S \cdot x) = O(A_L)$, φ_L^S and φ_S^S are the free-surface velocity potential components for the long and the short wave accordingly. As it is shown above the terms that are proportional to $A_L \cdot k_S$ exactly cancel. Therefore, the final expression of $\varphi_z(x, z = \eta(x,t), t)$ is given by

$$\varphi_z = \varphi_L^S \cdot k_L \left(1 + \eta^2 \cdot k_L^2 - \eta \cdot k_L\right) \sin\left(k_L \cdot x\right) + \varphi_S^S \cdot k_S \sin\left(k_S \cdot x\right).$$

The numerical verification of this argument however, can be proven only if all terms of the Taylor expansion are maintained. However, this is not plausible in a numerical sense. In order to validate whether HOS can be used for the solution of NLSWI, we run a series of cases of two interacting waves of steepness $\varepsilon = A_L \cdot k_L = A_S \cdot k_S = 0.1$ to avoid limitations related to the use of the perturbation expansion. The results are shown in the following graphs. Initially, we worked on the case of $k_L/k_S = 0.1$. The original free-surface elevation η at $t = 0$ is shown below (Fig. 3.4).

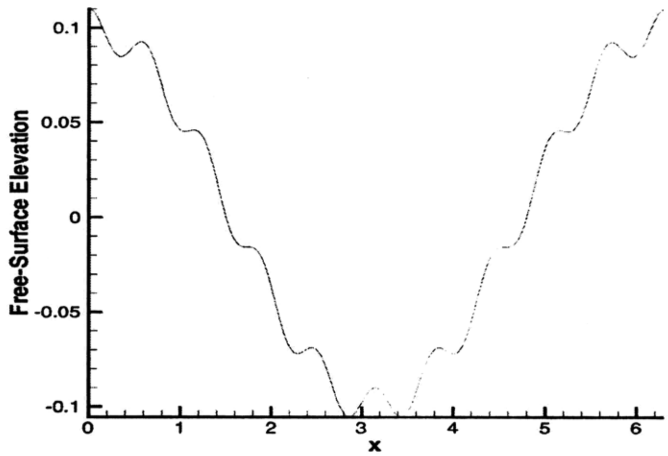

Figure 3-3: Initial condition of free-surface elevation for $k_L/k_S = 0.1$

After only about two time periods (t = 40 time steps), the free-surface vertical velocity calculations break due to the introduction of high harmonics. This is clear in the following figure (Fig. 3.4).

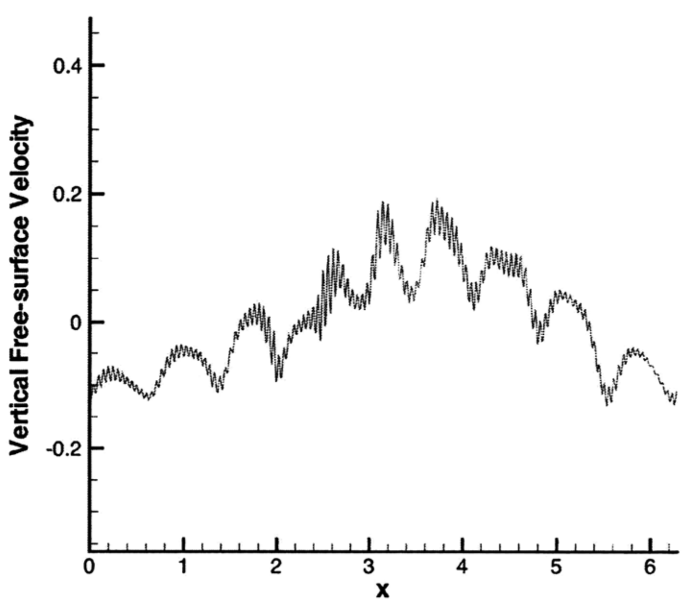

Figure 3-4: Free-surface vertical velocity at t = 39ts

The issues introduced in the former analysis can be resolved by applying at each time step a filter to eliminate non-physical frequencies that appear. This has been applied successfully in HOS for that reason we can treat case of $k_L/k_S = 0.1$. However, if we proceed in the case of $k_L/k_S = 0.01$ the former argument fails since we cannot distinguish between physical and non-physical frequencies that appear in the vertical velocity spectrum. In order to verify whether the results are physically meaningful, we run the some series of tests for different computer accuracy. The results showed that by changing the computational accuracy of the calculations different frequencies appear. The higher the computational accuracy the longer we can run the case to produce results.

Therefore, we conclude that:

- In principle mode-coupling methods can solve the problem of NLSWI, because the divergent terms introduced by the Taylor expansion about the mean free-surface analytically cancel

- In practice, however numerical results are limited by the computational precision, because divergent terms are first computed and then canceled causing computational errors to affect the results

In order to develop a new effective numerical method to treat the problem of interest, we need to eliminate the problems introduced by the divergent terms. Two different methods are proposed to overcome this difficulties. a) regrouping the computed terms of the free-surface vertical velocityφ_z so that the cancellation of divergent terms occurs intrinsically, before terms are calculated. This method has been investigated in order to produce an extension of HOS for NLWI. However, the special formulation of HOS prevents an effective regrouping of terms mainly because the computational efficiency of the method is severely damaged. For that reason we proceeded to the next option. b) development of a new method that avoids completely the Taylor expansion. In order to achieve that we will use a change of variables of the original problem. The next chapter deals with the mathematical formulation of NLSWI problem following the second proposition.

Chapter 4

Problem of Nonlinear Long-Short Wave Interactions (NLSWI)

4.1 Mathematical Formulation of NLSWI

4.1.1 Cartesian coordinates

We deal with an homogeneous, incompressible and inviscid fluid for the case of 2D, irrotational flow in deep water regime under a free-surface with periodic boundary conditions in x. The first step is to divide the fluid domain into two separate subdomains. The upper fluid domain (Domain I) includes the free-surface up to a depth h from the mean free-surface $z = 0$. The velocity potential in Domain I is denoted by φ. The lower fluid domain (Domain II) includes the rest lower part starting at $z = -h$.In Domain II the velocity potential is denoted by ϕ. The governing equation in the upper domain is given by

$$\nabla^2 \varphi \left(x, z, t\right) = 0, \tag{4.1}$$

where $x \in [0, 2\pi]$, $z \in [-h, \eta(x,t)]$, and φ is again the velocity potential. Using Zakharov's description for the boundary conditions at the free-surface $z = \eta(x,t)$, we have

$$\eta_t + \varphi_x^S \cdot \eta_x - \left(1 + \eta_x^2\right) \cdot \varphi_z = 0, \tag{4.2a}$$

$$\varphi_t + g\eta + \frac{1}{2}\left(\varphi_x^S\right)^2 - \frac{1}{2}\left(1+\eta_x^2\right)\cdot\left(\varphi_z\right)^2 = 0, \tag{4.2b}$$

where $\varphi^S = \varphi\left(x, \eta\left(x,t\right), t\right)$ is the free-surface velocity potential and g is the acceleration of gravity.

In domain II, the governing equation is equivalently given by

$$\nabla^2\phi\left(x,z,t\right) = 0, \tag{4.3}$$

where $x \in [0, 2\pi]$, $z \in [-\infty, -h]$.

At the interface $z = -h$, we have the following matching conditions

$$\varphi\left(x, z=-h\right) = \phi\left(x, z=-h\right), \tag{4.4a}$$

$$\varphi_z\left(x, z=-h\right) = \phi_z\left(x, z=-h\right). \tag{4.4b}$$

4.1.2 Transformation of the fluid domain

For the upper domain, we will employ a transformation of variables to simplify the problem's geometry. Initially we try the following change of variables

$$\widetilde{x} = x, \tag{4.5a}$$

$$\widetilde{z} = \frac{z-\eta\left(x,t\right)}{\eta\left(x,t\right)+h}, \tag{4.5b}$$

in order to map the original, complex, upper fluid domain into a simple rectangular domain, i.e. $(\widetilde{x}, \widetilde{z}) \in [0, 2\pi] \times [-1, 0]$. However this transformation is appropriate one. This is because in the limiting case for $h \to \infty$, the transformation maps the continuous interval $[-h, \eta]$ on a single point. Therefore, this transformation is not appropriate for our analysis. Instead we shall employ the following transformation

$$\widehat{x} = x, \tag{4.6a}$$

$$\widetilde{z} = h \cdot \frac{z - \eta(x,t)}{\eta(x,t) + h}, \tag{4.6b}$$

that maps the original Cartesian domain $(x, z) \in [0, 2\pi] \times [-h, \eta(x,t)]$ into the rectangular domain $(\widehat{x}, \widehat{z}) \in [0, 2\pi] \times [-h, 0]$. This transformation was also used for the solution of optics problems (Nicholls & Reitich 2004).

4.2 Transformed governing equations and boundary conditions

By applying the transformation given in Eq. (4.6a), (4.6b) in the upper domain, we manage to produce a simpler computational domain (see Fig. 4-1). However, the description of the problem, becomes more complex.

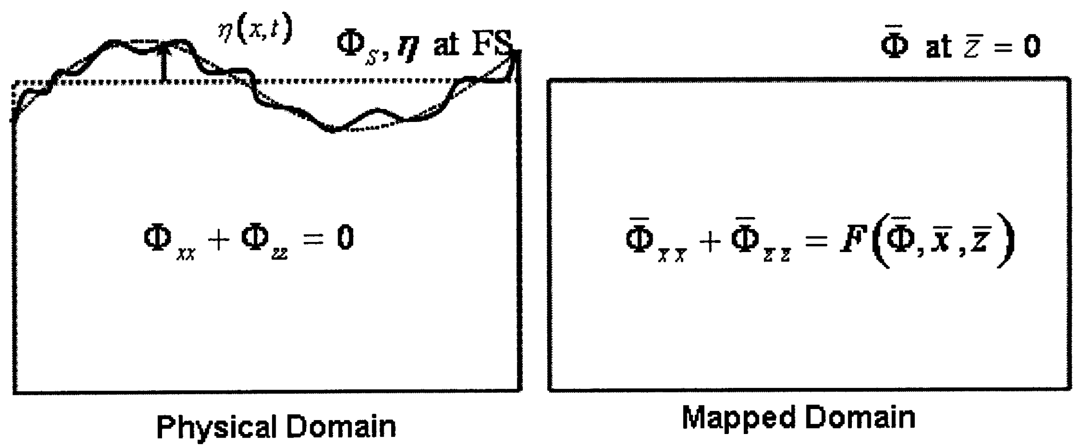

Figure 4-1: Transformation of original Cartesian domain of unsteady geometry into a simple, steady, computational domain

To be more specific, (C.3) becomes

$$\nabla^2 \widehat{\varphi}(\widehat{x}, \widehat{z}, t) = F(\widehat{\varphi}, \eta(\widehat{x}, t), \widehat{z}), \tag{4.7}$$

where

$$F(\widehat{\varphi},\widehat{\eta},\widehat{z}) = \frac{1}{h^2}(-\widehat{\eta}^2-2\widehat{\eta}h)\frac{\partial^2\widehat{\varphi}}{\partial\widehat{x}^2}-\frac{1}{h^2}(\widehat{\eta}_{\widehat{x}})^2(\widehat{z}+h)^2\frac{\partial^2\widehat{\varphi}}{\partial\widehat{z}^2} \tag{4.8}$$
$$+\frac{2}{h^2}\widehat{\eta}_{\widehat{x}}(\widehat{z}+h)(\widehat{\eta}+h)\frac{\partial^2\widehat{\varphi}}{\partial\widehat{x}\partial\widehat{z}}+\frac{1}{h^2}[\widehat{\eta}_{\widehat{x}\widehat{x}}(\widehat{z}+h)(\widehat{\eta}+h)-2(\widehat{\eta}_{\widehat{x}})^2(\widehat{z}+h)]\frac{\partial\widehat{\varphi}}{\partial\widehat{z}},$$

and $\widehat{\eta}=\eta(\widehat{x},t)$ is the free-surface in the transformed domain.

The kinematic boundary condition (C.1) and dynamic boundary condition (A.2) change accordingly as shown below

$$\widehat{\eta}_t(\widehat{\eta}+h)+\widehat{\eta}_{\widehat{x}}(\widehat{\eta}+h)\frac{\partial\widehat{\varphi}^S}{\partial\widehat{x}}-[(\widehat{\eta}_{\widehat{x}})^2\widehat{z}+2h(\widehat{\eta}_{\widehat{x}})^2+h]\frac{\partial\widehat{\varphi}}{\partial\widehat{z}}=0, \tag{4.9a}$$

$$\widehat{\varphi}_t^S(\widehat{\eta}+h)^2+(\widehat{\eta}+h)^2g\eta+\frac{1}{2}(\widehat{\eta}+h)^2\left(\frac{\partial\widehat{\varphi}^S}{\partial\widehat{x}}\right)^2-\widehat{\eta}_{\widehat{x}}(\widehat{z}+h)(\widehat{\eta}+h)\frac{\partial\widehat{\varphi}^S}{\partial\widehat{x}}\frac{\partial\widehat{\varphi}}{\partial\widehat{z}}+$$

$$+\frac{1}{2}[(\widehat{\eta}_{\widehat{x}})^2(\widehat{z}+h)^2-h^2\left(1+(\widehat{\eta}_{\widehat{x}})^2\right)]\left(\frac{\partial\widehat{\varphi}}{\partial\widehat{z}}\right)^2=0. \tag{4.10}$$

Domain II is described by the velocity potential ϕ as given in (4.3), with (4.4a) and (4.4b) being the matching conditions at the interface $z=-h$. This problem can be solved completely in the transformed domain using the above transformed free-surface boundary conditions. However, in this analysis we will not employ the transformed free-surface boundary conditions to obtain the time history of the free-surface elevation and free-surface velocity potential. Instead, we will use the original evolution equations after calculating the free-surface vertical velocity in the mapped domain.

4.3 Multi-scale method for the solution of the joint problem

We expand the free-surface velocity potential $\widehat{\varphi}$ in orders of ε. Therefore, we have

$$\widehat{\varphi}(\widehat{x},\widehat{z},t)=\sum_{m=1}^{M}\widehat{\varphi}_{(m)}(\widehat{x},\widehat{z},t). \tag{4.11}$$

The free-surface elevation $\widehat{\eta}$ is considered to be of order ε.Thus, the first order problem of the upper domain turns out to be

$$\nabla^2 \widehat{\varphi}_{(1)}(\widehat{x}, \widehat{z}, t) = 0, \tag{4.12}$$

with associated boundary condition (C.1) at the free-surface

$$\widehat{\eta}_t - \frac{\partial \widehat{\varphi}_{(1)}}{\partial \widehat{z}} = 0 \tag{4.13a}$$

$$\frac{\partial \widehat{\varphi}^S_{(1)}}{\partial t} + g\widehat{\eta} = 0. \tag{4.13b}$$

Accordingly, the lower domain problem is given by

$$\nabla^2 \phi_{(1)}(x, z, t) = 0, \tag{4.14}$$

where $x \in [0, 2\pi]$, $z \in [-\infty, -h]$.

At the interface $z = -h$ we have the following matching conditions

$$\varphi_{(1)}(x, z = -h) = \phi_{(1)}(x, z = -h), \tag{4.15a}$$

$$\frac{\partial \varphi_{(1)}}{\partial z}(x, z = -h) = \frac{\partial \phi_{(1)}}{\partial z}(x, z = -h), \tag{4.15b}$$

where the matching between the two domains is implemented after computing $\varphi_{(1)}(x, z = -h)$ and $\frac{\partial \varphi_{(1)}}{\partial z}(x, z = -h)$ using the inverse transformation in the original Cartesian domain.

The second order problem of the upper domain is given by

$$\nabla^2 \widehat{\varphi}_{(2)}(\widehat{x}, \widehat{z}, t) = f\left(\widehat{\varphi}_{(1)}, \widehat{\eta}, \widehat{x}, \widehat{z}\right), \tag{4.16}$$

where

$$f\left(\widehat{\varphi}_{(1)}, \widehat{\eta}, \widehat{x}, \widehat{z}\right) = -\frac{2}{h}\widehat{\eta}\frac{\partial \widehat{\varphi}_{(1)}}{\partial \widehat{x}} + \frac{2}{h}\widehat{\eta}_{\widehat{x}}(\widehat{z} + h)\frac{\partial^2 \widehat{\varphi}_{(1)}}{\partial \widehat{x}\partial \widehat{z}} + \frac{1}{h}\widehat{\eta}_{\widehat{x}\widehat{x}}(\widehat{z} + h)\frac{\partial \widehat{\varphi}_{(1)}}{\partial \widehat{z}} \tag{4.17}$$

.

and the associated kinematic and dynamic boundary conditions are formed by keeping terms up to second order.

$$\widehat{\eta}_t + \frac{1}{h}\widehat{\eta}_t\widehat{\eta} + \widehat{\eta}_{\widehat{x}}\frac{\partial \widehat{\varphi}^S_{(1)}}{\partial \widehat{x}} - \frac{\partial \widehat{\varphi}_{(2)}}{\partial \widehat{z}} = 0, \tag{4.18a}$$

$$\frac{\partial \widehat{\varphi}^S_{(2)}}{\partial t}h^2 + 2\frac{\partial \widehat{\varphi}^S_{(1)}}{\partial t}\widehat{\eta}h + h^2 g\eta + 2\left(\widehat{\eta}\right)^2 hg + \frac{1}{2}h^2\left(\frac{\partial \widehat{\varphi}^S_{(1)}}{\partial \widehat{x}}\right)^2 + \frac{1}{2}h^2\left(\frac{\partial \widehat{\varphi}_{(1)}}{\partial \widehat{z}}\right)^2 = 0. \tag{4.18b}$$

Accordingly, the lower domain problem is given by

$$\nabla^2 \phi_{(2)}\left(x, z, t\right) = 0, \tag{4.19}$$

where $x \in [0, 2\pi]$, $z \in [-\infty, -h]$.

At the interface $z = -h$ we the following matching conditions

$$\varphi_{(2)}\left(x, z = -h\right) = \phi_{(2)}\left(x, z = -h\right), \tag{4.20a}$$

$$\frac{\partial \varphi_{(2)}}{\partial z}\left(x, z = -h\right) = \frac{\partial \phi_{(2)}}{\partial z}\left(x, z = -h\right), \tag{4.20b}$$

where the matching between the two domains is implemented after computing $\varphi_{(2)}\left(x, z = -h\right)$ and $\frac{\partial \varphi_{(2)}}{\partial z}\left(x, z = -h\right)$ using the inverse transformation in the original Cartesian domain. We proceed with another approach that first focuses on the upper domain. We formulate and solve the boundary value problem in the mapped domain (Domain I). After obtaining the velocity potential in the mapped domain, we employ the inverse transformation to evaluate the free-surface vertical velocity φ_z. After the evaluation of φ_z, we use the kinematic and dynamic boundary conditions to evaluate the free-surface velocity potential and the free-surface elevation at the next time step. In order to solve the problem, we will use a perturbation expansion of the velocity potential $\widehat{\varphi}$. We also assume that the free-surface $\widehat{\eta}$ is of order ε. For the upper domain we have

$$\widehat{\varphi}\left(\widehat{x}, \widehat{z}, t\right) = \sum_{m=1}^{M} \widehat{\varphi}_{(m)}\left(\widehat{x}, \widehat{z}, t\right), \tag{4.21}$$

The first order problem of the upper domain governing equation turns out to be

$$\nabla^2 \widehat{\varphi}_{(1)}\left(\widehat{x}, \widehat{z}, t\right) = 0, \tag{4.22}$$

with associated boundary condition.

Accordingly, the lower domain problem is given by

$$\nabla^2 \phi_{(1)}(x, z, t) = 0, \tag{4.23}$$

where $x \in [0, 2\pi]$, $z \in [-\infty, -h]$.

At the interface $z = -h$ we have the following matching conditions

$$\varphi_{(1)}(x, z = -h) = \phi_{(1)}(x, z = -h), \tag{4.24a}$$

$$\frac{\partial \varphi_{(1)}}{\partial z}(x, z = -h) = \frac{\partial \phi_{(1)}}{\partial z}(x, z = -h),$$

where the matching between the two domains is implemented after computing $\varphi_{(1)}(x, z = -h)$ and $\varphi_z^{(1)}(x, z = -h)$ using the inverse transformation in the original Cartesian domain.

The second order problem of the upper domain is given by

$$\nabla^2 \widehat{\varphi}_{(2)}(\widehat{x}, \widehat{z}, t) = f\left(\widehat{\varphi}_{(1)}, \widehat{\eta}, \widehat{x}, \widehat{z}\right), \tag{4.25}$$

where

$$f\left(\widehat{\varphi}_{(1)}, \widehat{\eta}, \widehat{x}, \widehat{z}\right) = -\frac{2}{h}\widehat{\eta}\frac{\partial \widehat{\varphi}_{(1)}}{\partial \widehat{x}} + \frac{2}{h}\widehat{\eta}\left(\widehat{z} + h\right)\frac{\partial^2 \widehat{\varphi}_{(1)}}{\partial \widehat{x} \partial \widehat{z}} + \frac{1}{h}\widehat{\eta}_{\widehat{x}\widehat{x}}\left(\widehat{z} + h\right)\frac{\partial \widehat{\varphi}_{(1)}}{\partial \widehat{z}}. \tag{4.26}$$

In order to complete the description of the problem we need the associated boundary conditions in the free-surface and the interface.

At the interface $z = -h$ we the following matching conditions

$$\varphi_{(2)}(x, z = -h) = \phi_{(2)}(x, z = -h), \tag{4.27a}$$

$$\frac{\partial \varphi_{(2)}}{\partial z}(x, z = -h) = \frac{\partial \phi_{(2)}}{\partial z}(x, z = -h), \tag{4.27b}$$

where the matching between the two domains is implemented after computing $\varphi_{(2)}(x, z = -h)$ and $\frac{\partial \varphi_{(2)}}{\partial z}(x, z = -h)$ using the inverse transformation in the original Cartesian domain. For every order we solve the boundary value problem with the associated boundary condition at the free-surface and at the interface. After solving the boundary value problem, we proceed with the calculation of the free-surface vertical velocity at the physical domain with respect to the mapped domain velocity potential. We then use the free-surface dynamic and kinematic conditions in the original Cartesian domain to calculate the free-surface velocity potential ϕ^S and the free-surface elevation η at the next time step.The lower domain is not of interest in this study, therefore we will only focuss in the solution of the upper domain.

Chapter 5

New Numerical Method

5.1 Development process

The process of the solution of the problem of nonlinear long-short wave interactions is developed in a number of steps. In order to succeed in solving the NLSWI problem we need to develop a numerical method that sequentially solves the following subproblems.

- Solution of the Poisson's equation in the mapped domain for given boundary conditions of $\widehat{\varphi}$ at $\widehat{z} = 0$.
- Calculation of the free-surface vertical velocity, φ_z in the physical domain, with respect to the mapped domain velocity potential $\widehat{\varphi}$.
- Given φ_z calculate η, φ^S for the next time step employing HOS.
- Iteration of the above procedure to produce the time series of η, φ^S.

In this chapter we will elaborate on the method used for each step. As far as the first part is concerned, we performed a survey of available methods to choose a customized and efficient method for the solution each subproblem.

5.2 2D Poisson Solver

The first step of the problem of NLSWI is the solution of the Poisson equation on the mapped domain. For the solution to the Poisson equation in the mapped domain we have investigated several different numerical techniques. We have developed those numerical schemes with the objective to solve the general case of the Poisson equation for arbitrary forcing and given boundary conditions. The main goal is to be able to treat the problem in the mapped domain as it was described in the fourth chapter, in order to obtain the mapped velocity potential. Given that we will proceed using the inverse transformation for the evaluation of the free-surface vertical velocity in the mapped domain.

5.2.1 Finite-difference Poisson solver

Initially, we worked on a finite-difference numerical solution of the Poisson equation in the mapped domain. These methods are standard techniques for the solution of ordinary and partial differential equations. The implementation of the investingating numerical scheme was performed using a second order method. In a typical finite-difference scheme, we approximate the exact solution at a set of equally spaced points. Although, this method is simple and straight-forward to implement, there are several disadvantages that prohibit their use in the problem of interest.

The disadvantages of the finite-difference methods are:

- Low accuracy of the scheme
- Sensitive to boundary conditions
- For given number of iterations poorer results as the grid becomes finer
- Computationally expensive due to inverting very large, full matrices

Because of the above mentioned reasons we concluded that the use of this type of numerical solution is insufficient for the treatment of NLSWI problem. Thus, we proceeded to the study towards a spectral numerical scheme.

5.2.2 Spectral method Poisson solver

Spectral methods and pseudospectral methods are based on orthogonal expansions. The function is represented by an infinite expansion, $u\left(x\right) = \sum\limits_{k=0}^{\infty} c_k \cdot S_k\left(x\right)$, where $S_k\left(x\right)$ is the basis function that is used to represent the solution. The objective in spectral and pseudospectral methods is to estimate the coefficients c_k. The spectral methods outrival the finite-differences methods since they provide a global solution throughout the domain of integration in comparison to the finite differences schemes that require interpolation in order to calculate the value of the function in any intermediate point. Pseudospectral methods on the other hand, use the infinite expansion but provide as a result the values of the function $u(x)$ at $K+1$ discrete points $\{x_j\}$. The discrete points spacing is usually not equally spaced, because of advantages that different spacings offer. The most common spectral methods are based on Fourier series

$$u(x) = \frac{1}{2}a_0 + \sum_{k=1}^{\infty} (a_k \cdot \sin(kx) + b_k \cos(kx)). \tag{5.28}$$

Fourier methods are well-suited for periodic problems, however in non-periodic problems other bases can be considered. In the analysis that follows we will be using Chebyshev polynomials $T_k(x)$ defined in the interval $x \in [-1,1]$ for the representation of the basis function.

Chebyshev polynomials

There are four different kinds of Chebyshev polynomials.

- The Chebychev polynomial T_k of the first kind of degree k is defined as follows

$$T_k(x) = \cos(n\theta), \qquad \text{where } x = \cos\theta \text{ with } x \in [-1,1] \text{ and } \theta \in [0,\pi]. \tag{5.29}$$

- The Chebychev polynomial U_k of the second kind of degree k is defined as follows

$$U_k(x) = \sin((n+1)\theta) / \sin\theta, \qquad \text{where } x = \cos\theta \text{ with } x \in [-1,1] \text{ and } \theta \in [0,\pi]. \tag{5.30}$$

- The Chebychev polynomial V_k of the third kind of degree k is defined as follows

$$V_k(x) = \cos\left(\left(n + \frac{1}{2}\right)\theta\right) / \cos\frac{\theta}{2}, \qquad \text{where } x = \cos\theta \text{ with } x \in [-1,1] \text{ and } \theta \in [0,\pi]. \tag{5.31}$$

- The Chebychev polynomial W_k of the fourth kind of degree k is defined as follows

$$W_k(x) = \sin\left(\left(n+\frac{1}{2}\right)\theta\right) / \sin\frac{\theta}{2}, \qquad \text{where } x = \cos\theta \text{ with } x \in [-1,1] \text{ and } \theta \in [0,\pi]. \tag{5.32}$$

Recurrence relations

For every Chebyshev kind there is a recurrence relation that along with initial conditions can provide the Chebyshev polynomials up to an arbitrary order K. These relations are given below for all the different kinds of Chebyshev polynomials.

- First-kind Chebyshev polynomials T_k , recurrence relationship

$$T_k(x) = 2xT_{k-1}(x) - T_{k-2}(x), \qquad n = 2,3,... \tag{5.33}$$

with initial conditions

$$T_0(x) = 1, \quad T_1(x) = x. \tag{5.34}$$

- Second-kind Chebyshev polynomials U_k , recurrence relation

$$U_k(x) = 2xT_{k-1}(x) - T_{k-2}(x), \qquad n = 2,3,... \tag{5.35}$$

with initial conditions

$$U_0(x) = 1, \quad U_1(x) = 2x. \tag{5.36}$$

- Third-kind Chebyshev polynomials V_k , recurrence relation

$$V_k(x) = 2xV_{k-1}(x) - V_{k-2}(x), \qquad n = 2,3,... \tag{5.37}$$

with initial conditions

$$V_0(x) = 1, \quad V_1(x) = 2x - 1. \tag{5.38}$$

- Forth-kind Chebyshev polynomials W_k , recurrence relation

$$W_k(x) = 2xW_{k-1}(x) - W_{k-2}(x), \qquad n = 2, 3, ... \tag{5.39}$$

with initial conditions

$$W_0(x) = 1, \quad W_1(x) = 2x + 1. \tag{5.40}$$

For the rest of the analysis we use Chebychev polynomials of the first kind. However, there exist relations that connect the expressions of the four kinds of Chebyshev polynomials. This means that we can employ all four kinds of polynomials equivalently. For the remaining analysis we shall employ Chebychev polynomials of the first type for the expansion $u(x) = \sum_{k=0}^{K} c_k \cdot T_k(x)$

Integral of a Chebyshev expansion

Suppose we need to evaluate the indefinite integral of the following Chebyshev expansion series

$$f_K(x) = \sum_{k=0}^{K} c_k \cdot T_k(x), \tag{5.41}$$

where $f_K(x)$ is a $K-$th order polynomial.

The following integral

$$I_{k+1}(x) = \int f_K(x)\, dx = \sum_{k=0}^{K+1} C_k^{int} \cdot T_k(x) \tag{5.42}$$

where $I_{k+1}(x)$ is a $(K+1)-$th order polynomial.

The coefficients C_k^{int} are expressed in terms of the original coefficients c_k as follows

$$C_k^{int} = \frac{c_{k-1} - c_{k+1}}{2k}, \quad k > 0, \tag{5.43}$$

with $c_{k+1} = c_{k+2} = 0$ and C_0^{int} determined from the constant of integration. Therefore, there is an expression that allows us to obtain the coefficients of the integral of a Chebyshev expansion, given the coefficients of the original Chebyshev series.

Derivative of a Chebyshev expansion

Suppose we need to evaluate the derivative of the following Chebyshev expansion series

$$f_K(x) = \sum_{k=0}^{K} c_k \cdot T_k(x),$$

where $f_K(x)$ is a $K-$th order polynomial.

The derivative of the above series is given by

$$D_{k-1}(x) = \frac{d}{dx} f_K(x) = \sum_{k=0}^{K-1} C_k^{der} \cdot T_k(x) \tag{5.44}$$

where $D_{k-1}(x)$ is a $(K-1)-$th order polynomial.

The coefficients C_k^{der} are expressed in terms of the original coefficients c_k as follows

$$C_r^{der} = \sum_{\substack{k=r+1 \\ (k-r)\ odd}}^{K+1} 2k \cdot c_k. \tag{5.45}$$

Solution of Ordinary Differential Equation using Chebyshev polynomials of first kind

As we mentioned before finite-differences schemes are usually used for the numerical solution of ordinary differential equations (ODE). However, due to important drawbacks of this type of numerical methods, we turned to spectral methods for the treatment of ordinary differential equations. More specifically, we will be using a Collocation method with Chebyshev polynomials for the solution of the problem of interest. More detailed information on different types of spectral methods are available in the books of Gottlieb & Orszag 1993 and Canuto, Hussaini & Quateroni 1987.

In order to use this method for the solution of the problem of interest, we need to address two important issues. a) introduction of boundary conditions into the solution, b) calculation of spectral expansion coefficients. For non-periodic boundary conditions Chebyshev polynomials are a common choice. Chebychev polynomials do not satisfy boundary conditions but we can always add explicit constraints so that boundary conditions are satisfied.

We will explain the Chebyshev collocation method by using a simple example. Assume that we need to solve the following ordinary differential equation, $\frac{d^2}{dz^2}u(z) = f(z)$, $u(-1) = u(1) = 0$. The function $f(z)$ is expressed in the following form

$$u(z) = \sum_{k=0}^{\infty} c_k T_k(z).$$

In order to formulate the system of algebraic equation we need to use the following expression

$$\frac{d^2}{dz^2}T_k(z) = \sum_{\substack{r=0 \\ (k-r)\ even}}^{k-2} (k-r)\,k\,(k+r)\,T_r(z), \quad (k \geq 2).$$

Therefore, by substituting the above expressions in the governing equation and boundary conditions we obtain the following expressions

$$\sum_{k=0}^{\infty} \sum_{\substack{r=0 \\ (k-r)\ even}}^{k-2} (k-r)\,k\,(k+r)\,c_k T_r(z) = f(z),$$

$$\sum_{k=0}^{\infty} (-1)^k c_k = \sum_{k=0}^{\infty} c_k = 0.$$

Usually, we truncate the infinite sums to a maximum order K. In order to solve for the $K+1$ coefficients of the expansion we will use a collocation method. We select $K-1$ points, called collocation points $\{z_1, ..., z_{K-1}\}$ where $\frac{d^2}{dz^2}u(z_j) = f(z_j)$, $j = 1, ..., K-1$. We also have to extra equations that stem from the boundary conditions at $z = \pm 1$. We then end up to the following system of $K+1$ linear equations

$$\sum_{k=0}^{K} \sum_{\substack{r=0 \\ (k-r)\ even}}^{k-2} (k-r)\,k\,(k+r)\,c_k T_r(z_j) = f(z_j), \quad j = 1, ..., K-1 \tag{5.46}$$

$$\sum_{k=0}^{K} (-1)^k c_k = \sum_{k=0}^{K} c_k = 0. \tag{5.47}$$

We can reduce the above equations by choosing appropriately the collocation points. If for example we use as collocation points the zeros of Chebychev polynomials

$$z_j = \cos\frac{\left(j-\frac{1}{2}\right)\pi}{K-1}, \quad \text{with } \; j = 1, ..., K-1, \tag{5.48}$$

then employing discrete orthogonality relations we deduce the equation into

$$\sum_{\substack{k=l+2 \\ (k-r)\ even}}^{K} (k-r)\,k\,(k+r)\,c_k = \frac{2}{K-1}\sum_{j=1}^{K-1} T_l\left(z_j\right) f\left(z_j\right), \quad l = 0, ..., K-2, \tag{5.49}$$

along with the associated boundary conditions.

Specific problem of interest

As we mentioned before, we expand the velocity potential into orders and solve a boundary value problem for each order separately. After that we sum up results from each order. More specifically, assume that the velocity potential in the mapped domain is represented by a perturbation expansion in orders of $\varepsilon = Ak$, a measure of the relevant steepness of the problem

$$\widehat{\phi} = \sum_{m=1}^{M} \widehat{\phi}_{(m)}\left(\widehat{x}, \widehat{z}\right). \tag{5.50}$$

In order to solve Poisson's equation, we shall use Chebyshev expansion for the velocity potential in the vertical direction and Fourier expansion because we need to satisfy periodic boundary condition in the $x-$direction. Therefore, the velocity potential for each order m is represented by

$$\widehat{\phi}_{(m)}\left(\widehat{x}, \widehat{z}\right) = \sum_{n=0}^{N}\sum_{k=0}^{K} B_{nk}^{(m)} T_k\left(\widehat{z}\right) e^{in\widehat{x}}. \tag{5.51}$$

The expression of the velocity potential φ becomes

$$\widehat{\phi}\left(\widehat{x}, \widehat{z}\right) = \sum_{m=1}^{M}\sum_{n=0}^{N}\sum_{k=0}^{K} B_{nk}^{(m)} T_k\left(\widehat{z}\right) e^{in\widehat{x}}. \tag{5.52}$$

We form the boundary value problem for each order.

Namely, for $m = 1$, the governing equation within the fluid domain is Laplace's equation

$$\nabla^2 \widehat{\phi}_{(1)} = F_{(1)} = 0, \tag{5.53}$$

with the associated boundary condition

$$\widehat{\phi}_{(1)}\left(\widehat{x}, \widehat{z} = 0\right) = \widehat{\phi}^S = given, \tag{5.54}$$

$$\frac{\partial \widehat{\phi}_{(1)}}{\partial \widehat{z}}\left(\widehat{x}, \widehat{z} = -h\right) = .given. \tag{5.55}$$

The second order problem $m = 2$, is formulated accordingly

$$\nabla^2 \widehat{\phi}_{(2)} = F_{(2)}\left(\widehat{\phi}_{(1)}, \widehat{x}, \widehat{z}\right), \tag{5.56}$$

where $F_{(2)}\left(\widehat{\phi}_{(1)}, \widehat{x}, \widehat{z}\right) = -\frac{2}{h}\widehat{\eta}\frac{\partial \widehat{\varphi}_{(1)}}{\partial \widehat{x}} + \frac{2}{h}\widehat{\eta}\left(\widehat{z} + h\right)\frac{\partial^2 \widehat{\varphi}_{(1)}}{\partial \widehat{x}\partial \widehat{z}} + \frac{1}{h}\widehat{\eta}_{\widehat{x}\widehat{x}}\left(\widehat{z} + h\right)\frac{\partial \widehat{\varphi}_{(1)}}{\partial \widehat{z}}$ and with the associated boundary condition

$$\widehat{\phi}_{(2)}\left(\widehat{x}, \widehat{z} = 0\right) = 0, \tag{5.57}$$

$$\frac{\partial \widehat{\phi}_{(2)}}{\partial \widehat{z}}\left(\widehat{x}, \widehat{z} = -h\right) = .given. \tag{5.58}$$

The higher order problems are formulated in the same way

$$\nabla^2 \widehat{\phi}_{(m)} = F_{(m)}\left(\widehat{\phi}_{(1)}, \widehat{\phi}_{(2)}, ..., \widehat{\phi}_{(m-1)}, \widehat{x}, \widehat{z}\right), \tag{5.59}$$

with the associated boundary condition

$$\widehat{\phi}_{(m)}\left(\widehat{x}, \widehat{z} = 0\right) = 0, \tag{5.60}$$

$$\frac{\partial \widehat{\phi}_{(m)}}{\partial \widehat{z}}\left(\widehat{x}, \widehat{z} = -h\right) = .given. \tag{5.61}$$

Spectral Poisson solver

The first order problem is solved using the classical high order spectral method formulation. For each order of perturbation expansion $m > 1$, we have

$$\widehat{\phi}_{(m)}(\widehat{x},\widehat{z}) = \sum_{n=0}^{N}\sum_{k=0}^{K} B_{nk}^{(m)} T_k(\widehat{z})\, e^{in\widehat{x}}. \tag{5.62}$$

After substituting in the governing equation, we obtain

$$\sum_{n=0}^{N}\sum_{k=0}^{K} B_{nk}^{(m)} \left[\left(-n^2\right) T_k(\widehat{z})\, e^{in\widehat{x}} + T_k''(\widehat{z})\right] e^{in\widehat{x}} = F_{(m)}(\widehat{x},\widehat{z}). \tag{5.63}$$

Initially, we expand the forcing term in a Fourier series,

$$F_{(m)}(\widehat{x},\widehat{z}) = \sum_{n=0}^{N}\sum_{k=0}^{K} F_{m,n}(\widehat{z})\, e^{in\widehat{x}}. \tag{5.64}$$

Therefore, for every Fourier mode n, the problem formulation becomes

$$\sum_{k=0}^{K} B_{nk}^{(m)} \left[\left(-n^2\right) T_k(\widehat{z})\, e^{in\widehat{x}} + T_k''(\widehat{z})\right] = F_{m,n}(\widehat{z}), \tag{5.65}$$

with the associated boundary conditions $\widehat{\phi}_{(m)}(\widehat{x},\widehat{z}) = 0$, $\widehat{\phi}_{\widehat{z}}^{(m)}(\widehat{x},\widehat{z}) = .given$, at $z = 0$ and $z = -h$ accordingly. Therefore we formulate an algebraic system of $K+1$ equations the solution of which produces the amplitudes $B_{nk}^{(m)}$. After solving the problem for each order, we obtain the velocity potential in the mapped domain. The next step includes the calculation of the free-surface vertical velocity in the physical domain, by using the velocity potential we calculated in the mapped domain and the inverse transformation of variables.

Test cases of the Poisson solver

1D Case with homogeneous boundary conditions: The first problem that we will study is shown graphically below.

The forcing term is given by $f(z) = z^2$ and $k = 0, \ldots, K$. We will use Chebyshev expansion for the forcing term, $f(z) = \sum_k F_k T_k(z)$.

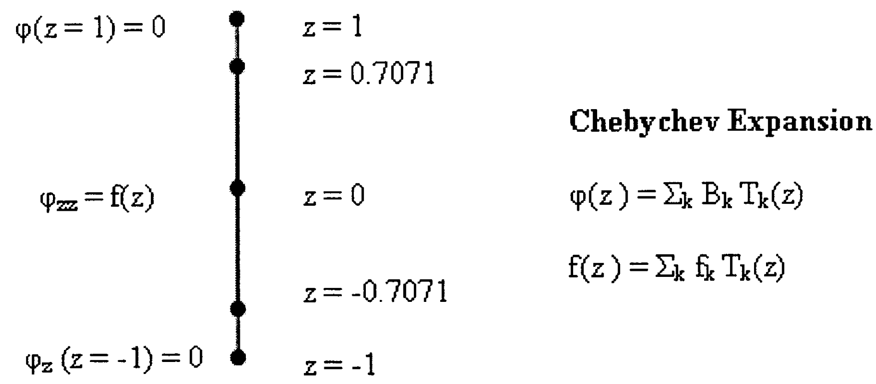

Figure 5-1: Schematic representation of the 1D problem

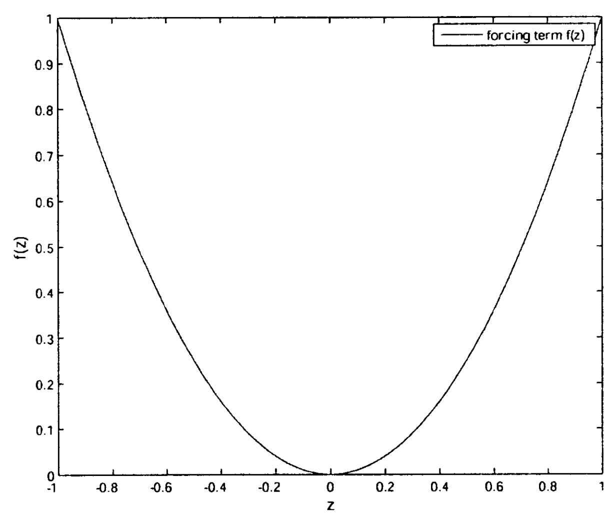

Figure 5-2: The forcing term $f(z)$ as fuction of z

The following table shows the forcing evaluated at the collocation points $z_j = cos(\pi j/K)$, where $K = 4$ is the maximum Chebyshev expansion order.

z	1	0.7071	0	-0.7071	-1
$f(z)$	1	0.5	0	0.5	1

Table 5-1: Values of forcing term at collocation points

The coefficients of the Chebyshev expansion of the forcing term $f(x)$ are given below

F_0	F_1	F_2	F_3	F_4
0.5	0	0.5	0	0

Table 5-2: Values of Chebyshev coefficient of the forcing term

The forcing is expressed by

$$f(z) = F_0 T_0(z) + F_1 T_1(z) + F_2 T_2(z) + F_3 T_3(z) + F_4 T_4(z),$$

where $T_0(z) = 1, T_1(z) = z, T_2(z) = 2z^2 - 1, T_3(z) = 4z^3 - 3z, T_4(z) = 8z^4 - 8z^2 + 1.$

The Chebyshev polynomials employed for the expansion are shown below.

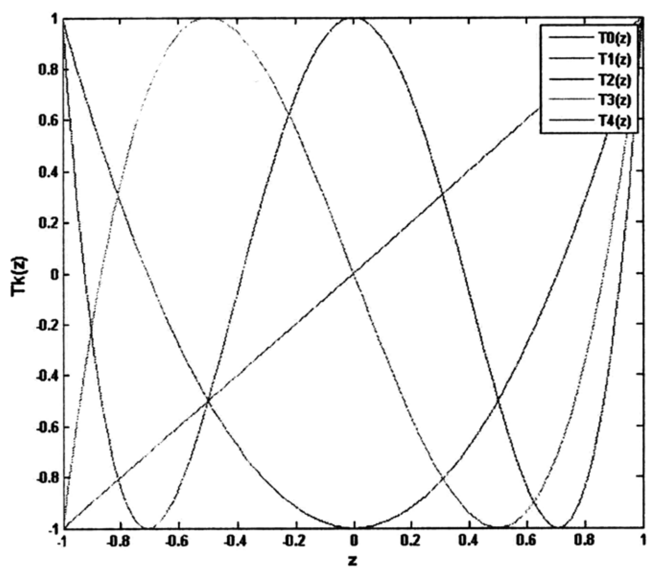

Figure 5-3: The Chebyshev polynomials $T_k(z)$ up to $K = 4$

The mathematical formulation of the spectral solver follows. The velocity potential is represented by the following expansion, $\varphi(z) = \sum_k B_k T_k(z)$. By substituting the former expansion in the governing equation $\varphi_{zz} = f(z)$, we obtain

$$\sum_k [B_k T_k'(z) - F_k T_k(z)] = 0, \quad k = 0, \ldots, K$$

The associated boundary condition at $z = 1$, $\varphi(1) = 0$ is given by

$$\sum_k B_k T_k(1) = 0, \quad k = 0, \dots, K$$

and at $z = -1, \varphi_z(-1) = 0$ is given by

$$\sum_k B_k T_k'(-1) = 0, \quad k = 0, \dots, K.$$

In order to solve the problem and calculate the coefficients B_k, $k = 0, \dots, K$, we formulate a system of algebraic equations on the form $Ax = b$, where

$$A = \begin{bmatrix} T_0(z_0) & T_1(z_0) & \cdots & T_K(z_0) \\ T_0''(z_1) & T_1''(z_1) & \cdots & T_K''(z_1) \\ & & \ddots & \\ T_0'(z_K) & T_1'(z_K) & \cdots & T_K'(z_K) \end{bmatrix} \quad x = \begin{bmatrix} B_0 \\ B_1 \\ \vdots \\ B_K \end{bmatrix} \quad b = \begin{bmatrix} f(z_0) \\ f(z_1) \\ \vdots \\ f(z_K) \end{bmatrix}$$

The points are the Gauss-Lobatto collocation points .The unknown B_k are calculated by solving the above system, $x = A^{-1}y$. For different values of K, we evaluate the error of the method. The collocation solution converges exponentially to the exact solution as the number of collocation points increases. The exact solution is given by $\varphi_{exact}(z) = \frac{1}{12}\left(z^4 - 1\right)$. In order to get the former conclusion, the same procedure has been followed for different values of K. The convergence behavior of the Spectral Poisson Solver with respect to K is demonstrated by the behavior of the maximum error of the solution as a function of K. The graph is given in linear-logarithmic scale to show the exponential behavior of the error.

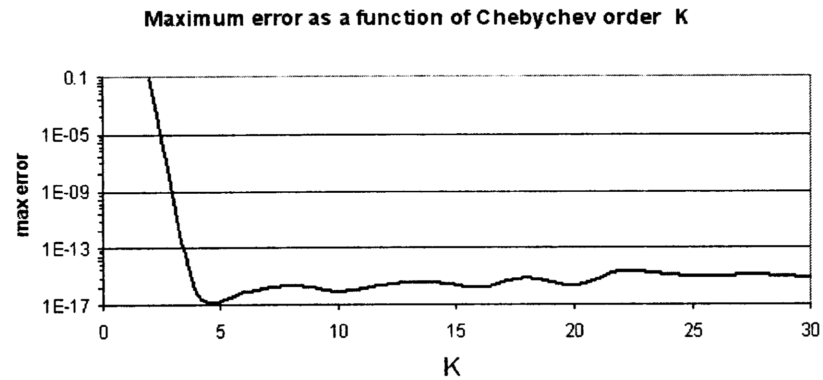

Figure 5-4: Maximum error as a function of Chebychev order K for $f(z) = z^2$

Therefore, we conclude that the spectral solver provides exponential convergence for the solution of the Poisson equation. We will apply the solver to another case, where the forcing, $f(x)$ is not represented by a finite number of Chebychev terms, $T_k(z)$. Let us assume that the forcing term is given by $f(x) = e^{4z}$, with homogeneous boundary conditions $\varphi(z = \pm 1) = 0$. Then, the exact solution is given by $\varphi_{exact}(z) = \frac{1}{16}\left(e^{4z} - z\sinh 4 - \cosh 4\right)$. After following the same procedure we end up with with the maximum error as a function of K. The convergence of the method to the exact solution is again exponential although more Chebychev terms are necessary to obtain it.

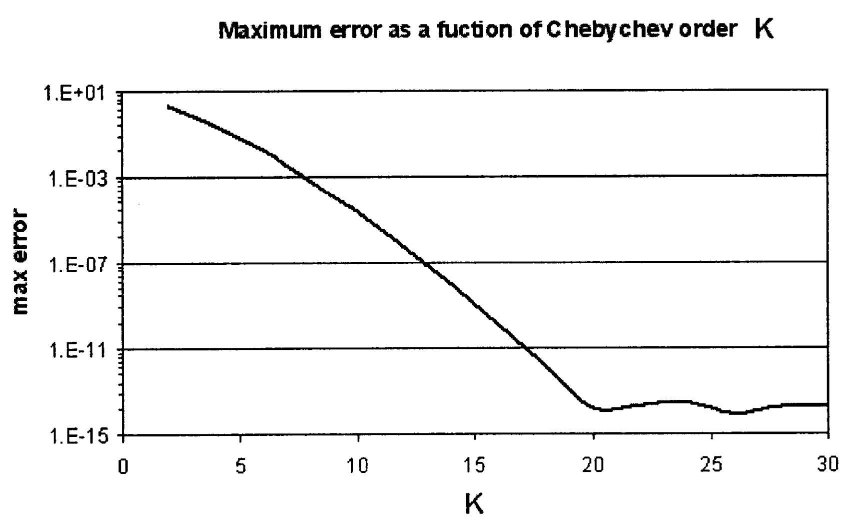

Figure 5-5: Maximum error as a function of Chebychev order K for $f(z) = e^{4z}$

2D Case with periodic boundary conditions in x-direction: In the cases of interest of this analysis, which is the solution of Poisson equation in the mapped domain, we have special characteristics that allow us for further assumptions. The problem remains periodic in x because of the specific transformation used and fluid domain is considered of constant depth. We proceed with the problem formulation for a specific case of boundary conditions $a(x)$ and forcing $f(x, z)$. The problem is shown graphically in the following figure.

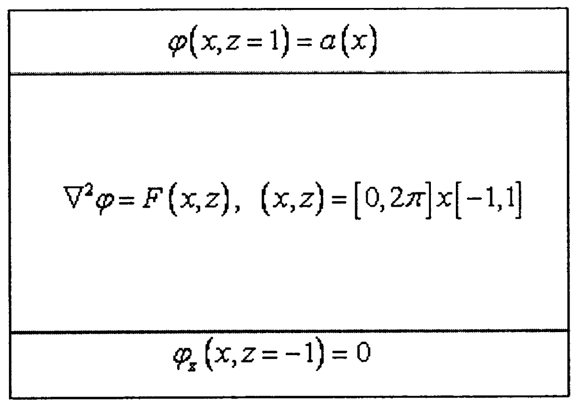

Figure 5-6: Schematic representation of the 2D problem

The computational domain is $(x, z) = [0, 2\pi]x[-1, 1]$. Let us assume for simplicity that the boundary condition at $z = 1$ is homogeneous, i.e. $a(x) = 0$ and the forcing term with in the fluid domain is $f(x, z)$. We assume that the velocity potential can then be expressed in the following manner.

$$\begin{aligned} \varphi(x, z) &= \sum_{n=0}^{N} A_n(z) \cdot e^{inx}, \\ A_n(z) &= \sum_{k=0}^{K} B_{nk} \cdot T_k(z). \end{aligned}$$

This leads to the following expression for the velocity potential within the fluid domain.

$$\varphi(x, z) = \sum_{n=0}^{N} \sum_{k=0}^{K} B_{nk} \cdot T_k(z) \cdot e^{inx}.$$

We then substitute this expression of the velocity potential in the governing equation, $\varphi_{xx} +$

$\varphi_{zz} = f(x,z)$ and we obtain.

$$\sum_{n=0}^{N}\sum_{k=0}^{K}\left[\left(-n^2\right)\cdot B_{nk}\cdot T_k(z)\cdot e^{inx} + B_{nk}\cdot T_k''(z)\cdot e^{inx}\right] = f(x,z).$$

We then express the forcing term $f(x,z)$ as follows

$$f(x,z) = \sum_{n=0}^{N} C_n(z)\cdot e^{inx}.$$

Therefore, for each Fourier mode n, we have to solve an ordinary differential equation only in z.

$$\sum_{k=0}^{K} B_{nk}\cdot\left[\left(-n^2\right)\cdot T_k(z) + T_k''(z)\right] = C_n(z)$$

Furthermore, since the expression of the Chebyshev base functions are known, the problem transforms into a system of algebraic equations of the form $Ax = b$, where x is the unknown coefficients of the velocity potential φ. We have $K+1$ unknown coefficients, therefore we need the same number of equations to obtain these coefficients. We select $K-1$ points $z = \{z_1, z_2, ...z_{K-1}\}$ and require the velocity potential to satisfy the governing equation. The two missing equations will come out of the boundary conditions at $z = -1, 1$.

The system of $K+1$ linear equations is given below

$$\sum_{k=2}^{K}\sum_{\substack{r=0\\(k-r)\ even}}^{k-2}(k-r)\,k\,(k+r)\,c_k T_r(x_j) = f(x_j), \qquad j = 1, ..., n-1$$

$$\varphi(x, z=-1) = \sum_{k=0}^{K} B_{nk}\cdot T_k(-1) = 0,$$

$$\varphi(x, z=1) = \sum_{k=0}^{K} B_{nk}\cdot T_k{}'(1) = 0.$$

Assuming that $f(x,z) = \sin x\cdot z^2$and $K = 5$. We first use Fourier expansion for the forcing term in the x-direction, $f(x,z) = \sum_{n=0}^{N}\sum_{k=0}^{K} F_{nk}\cdot T_k(z)\cdot e^{inx}$.

By substituting the expression of the velocity potential in the governing equation at $K-1$ collocation points we obtain $K-1$ equations. For this specific case $N=1$ and $K=5$, therefore we obtain four equations.

$$\sum_{k=1}^{K=4} B_{nk} \cdot \left[\left(-n^2\right) \cdot T_k(z) + T_k''(z)\right] = \sum_{k=1}^{K=4} F_{nk} \cdot T_k(z)$$
$$\sum_{k=1}^{K=4} B_{1k} \cdot \left[\left(-1^2\right) \cdot T_k(z) + T_k''(z)\right] = \sum_{k=1}^{K=4} F_{1k} \cdot T_k(z)$$

Expanding the previous sum, we obtain

$$B_{10} \cdot \left[\left(-1^2\right) \cdot T_0(z) + T_0''(z)\right] + B_{11} \cdot \left[\left(-1^2\right) \cdot T_1(z) + T_1''(z)\right] +$$
$$+B_{12} \cdot \left[\left(-1^2\right) \cdot T_2(z) + T_2''(z)\right] + B_{13} \cdot \left[\left(-1^2\right) \cdot T_3(z) + T_3''(z)\right] +$$

$$+B_{14} \cdot \left[\left(-1^2\right) \cdot T_4(z) + T_4''(z)\right] =$$

$$= F_{11} \cdot T_1(z) + F_{12} \cdot T_2(z) + F_{13} \cdot T_3(z) + F_{14} \cdot T_4(z).$$

We use $K-1$ Gauss-Lobatto collocation points $z_i = \cos\left(\frac{\pi i}{K}\right)$, $[z] = [z_0, ..., z_K]^T = [z_0, z_1, z_2, z_3, z_4]^T$. Therefore, the matrix A and the vector b are formulated as follows

$$A = \begin{bmatrix} T_0(z_1) & T_1(z_1) & T_2(z_1) & T_3(z_1) & T_4(z_1) \\ T_0''(z_1) - T_0(z_1) & T_1''(z_1) - T_1(z_1) & T_2''(z_1) - T_2(z_1) & T_3''(z_1) - T_3(z_1) & T_4''(z_1) - T_4(z_1) \\ T_0''(z_2) - T_0(z_2) & T_1''(z_2) - T_1(z_2) & T_2''(z_2) - T_2(z_2) & T_3''(z_2) - T_3(z_2) & T_4''(z_2) - T_4(z_2) \\ T_0''(z_3) - T_0(z_3) & T_1''(z_3) - T_1(z_3) & T_2''(z_3) - T_2(z_3) & T_3''(z_3) - T_3(z_3) & T_4''(z_3) - T_4(z_3) \\ T_0'(z_4) & T_1'(z_4) & T_2'(z_4) & T_3'(z_4) & T_4'(z_4) \end{bmatrix},$$

$$b = \begin{bmatrix} 0 \\ F_{10}T_1(z_1) + F_{11}T_1(z_1) + F_{12}T_2(z_1) + F_{13}T_3(z_1) + F_{14}T_4(z_1) \\ F_{10}T_1(z_2) + F_{11}T_1(z_2) + F_{12}T_2(z_2) + F_{13}T_3(z_2) + F_{14}T_4(z_2) \\ F_{10}T_1(z_3) + F_{11}T_1(z_3) + F_{12}T_2(z_3) + F_{13}T_3(z_3) + F_{14}T_4(z_3) \\ 0 \end{bmatrix}.$$

A number of different 2D cases with periodic boundary condition in the $x-$direction was solved successfully using the new Chebyshec-Fourier spectral solver. According to the results the spectral solver was found to be more appropriate than the finite-difference numerical scheme. This methods presents many advantages for the problem of interest. After establishing the type of Poisson solver that is going to be used, we can proceed to the calculation of the free-surface vertical velocity in the physical domain with respect to the velocity potential of the mapped domain. In the next paragraph, we will discuss about the calculation of the free-surface vertical velocity φ_z.

Chapter 6

Discussion

6.1 Set-up of test cases

After having developed the new Mapped-Domain Spectral Method (MDSM) we needed to compare its results with those obtained by a reliable method. The method used for that reason was HOS. The investigation and verification of MDSM was performed for a number of different cases. HOS was also simulated for the same number of cases and their results were compared. As initial conditions for the investigation we used linear expressions for the free-surface elevation and free-surface velocity potential.as shown below. We focused our study on the investigation of the linear and quadratic cases, i.e. $M = 1$ and $M = 2$ for the 2D, infinite depth problem water wave problem with initial condition at the free-surface where given by

$$\eta\left(x, t=0\right) = \sum_{n=1}^{N} A_n \cos\left(k_n x\right), \tag{6.1}$$

$$\varphi^S\left(x, t=0\right) = \sum_{n=1}^{N} \frac{A_n \omega_n}{k_n} \sin\left(k_n x\right). \tag{6.2}$$

For the study of two interacting waves, $N = 2$, the non-dimensional parameters of interest are two. The first one is $\varepsilon = kA$ representing the wave steepness of the long and short waves. In our analysis both waves have the same steepness, $A_L k_L = A_S k_S$. The second parameter is $\delta = \lambda_S/\lambda_L = k_L/k_S$. This is a length-scale parameter that indicates how small or large one wave is with respect to the other. The following table provides the nomenclature of the cases for which we shall simulate MDSM and HOS.

δ / ε	0.5	0.1	0.01	1
0.1	A_1	A_2	A_3	A_4
0.2	B_1	B_2	B_3	B_4
0.3	C_1	C_2	C_3	C_4

Table 6-1: Test cases classification table

More specifically, the wavelength of the long wave is considered for all cases to be equal to the computational domain length, $k_L = 1$. Also, the wave amplitude of the long waves is 0.1, 0.2, 0.3 for the A, B and C cases accordingly. As far as the short wave is concerned for each series A, B, and C the information is given below.

Case A	A_S	k_S	Case B	A_S	k_S	Case C	A_S	k_S
A_1	0.05	2	B_1	0.2	2	C_1	0.15	2
A_2	0.01	10	B_2	0.02	10	C_2	0.03	10
A_3	0.001	100	B_3	0.002	100	C_3	0.003	100
A_4	0.1	1	B_4	0.2	1	C_4	0.3	1

Table 6-2: Short wave characteristics for all test cases

6.2 Mapped-Domain Spectral Method (MDSM) results

Starting in the original computational domain, the problem is set as follows. The initial condition according to Eq. (6.1) and Eq. (6.2) are given by

$$\eta\left(x,t=0\right) = A_L \cos\left(k_L x\right) + A_S \cos\left(k_S x\right), \tag{6.3}$$

$$\varphi^S\left(x,t=0\right) = \frac{A_L \omega_L}{k_L} \sin\left(k_L x\right) + \frac{A_S \omega_S}{k_S} \sin\left(k_S x\right). \tag{6.4}$$

The original domain is shown below. This domain is changing with time as the free-surface changes with time. The free-surface elevation $\eta\left(x,t\right)$ and the free-surface velocity potential

$\varphi^S(x,t)$ at the initial time step contains only two wave modes, the short and the long one.

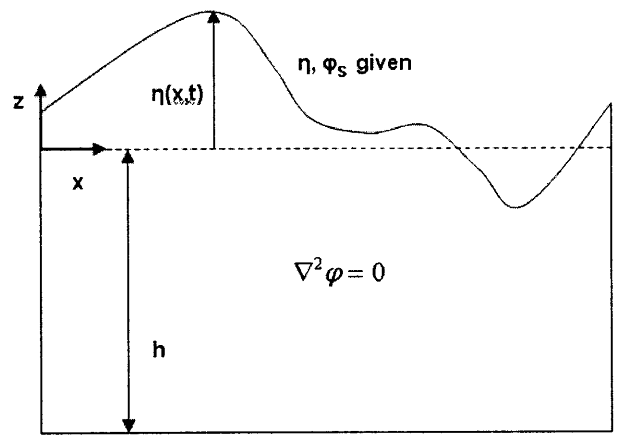

Figure 6-1: Problem set-up in Cartesian coordinates x, z

The specific values of A_L, k_L and A_S, k_S are given in the table above. The mapped domain remain unchanged as time pass as it is shown in the following graph.

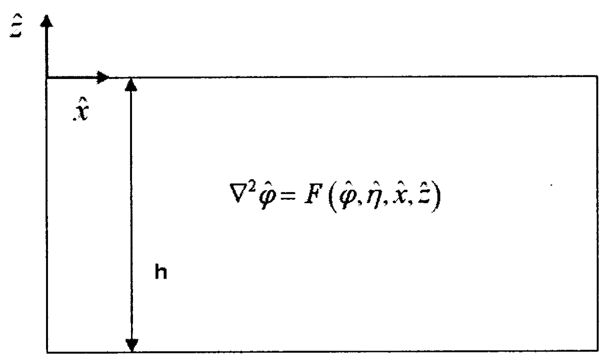

Figure 6-2: Problem set-up in transformed coordinates $\widehat{x}$, $\widehat{z}$

At first, we work on the mapped domain and solve sequentially the Poisson equation up to nonlinear order M. For this study we will work for up to second nonlinear order. For the first order problem Poisson's equation reduces to a Laplace equation. The second order problem is described accordingly.

For $m = 1$, the governing equation is

$$\nabla^2 \widehat{\phi}_{(1)} = F_{(1)} = 0, \tag{6.5}$$

with the associated boundary conditions

$$\widehat{\phi}_{(1)}\left(\widehat{x},\widehat{z}=0\right)=\widehat{\phi}^{S}, \tag{6.6}$$

$$\frac{\partial\widehat{\phi}_{(1)}}{\partial\widehat{z}}\left(\widehat{x},\widehat{z}=-h\right)=.given. \tag{6.7}$$

The second order problem $m=2$, is also given by

$$\nabla^{2}\widehat{\phi}_{(2)}=-\frac{2}{h}\widehat{\eta}\frac{\partial\widehat{\varphi}_{(1)}}{\partial\widehat{x}}+\frac{2}{h}\widehat{\eta}\left(\widehat{z}+h\right)\frac{\partial^{2}\widehat{\varphi}_{(1)}}{\partial\widehat{x}\partial\widehat{z}}+\frac{1}{h}\widehat{\eta}_{\widehat{x}\widehat{x}}\left(\widehat{z}+h\right)\frac{\partial\widehat{\varphi}_{(1)}}{\partial\widehat{z}}, \tag{6.8}$$

with the associated boundary condition

$$\widehat{\phi}_{(2)}\left(\widehat{x},\widehat{z}=0\right)=0, \tag{6.9}$$

$$\frac{\partial\widehat{\phi}_{(2)}}{\partial\widehat{z}}\left(\widehat{x},\widehat{z}=-h\right)=given. \tag{6.10}$$

Each problem for $M=1,2$ is solved individually and the results from each problem are summed to produce the total velocity potential in the mapped domain as shown in Eq. (6.11).

$$\widehat{\phi}=\widehat{\phi}_{(1)}+\widehat{\phi}_{(2)} \tag{6.11}$$

After solving the problem in the mapped domain, we need to proceed to the calculation of the free-surface vertical velocity φ_z.

6.3 Free-surface vertical velocity

According to the classical HOS method, the calculation of the free-surface vertical velocity is performed by solving the boundary value problem in the physical domain and using a Taylor expansion about the mean free-surface $z=0$. This methodology is proven to cause a number of issues related to the computer accuracy and convergence of the method as it was presented in earlier chapters. In order to avoid these problems, we are solving the boundary value problem for

$\widehat{\phi}$ in the steady, rectangular, mapped domain and then using $\widehat{\phi}$ we proceed with the evaluation of the free-surface vertical velocity φ_z in the physical domain. In order to better understand the procedure of this step, we need to analyze the transformation of variables used.

6.3.1 Transformation of variables

The transformation of variables used related the physical domain $(x, z) = [0, 2\pi]\, x\, [-h, \eta]$ with the mapped domain $(\widehat{x}, \widehat{z}) = [0, 2\pi]\, x\, [-1, 0]$. The mapping is described below

$$\begin{aligned} x &= \widehat{x} \\ z &= \widehat{z}(h + \eta) + \eta \end{aligned} \tag{6.12}$$

where η is the free-surface elevation and h is the mean depth of the original computational domain.

The inverse transformation from the mapped domain to the physical domain is given by

$$\begin{aligned} \widehat{x} &= x, \\ \widehat{z} &= \frac{z - \eta}{h + \eta} \end{aligned} \tag{6.13}$$

By using the chain rule, we obtain

$$\frac{\partial}{\partial x} = \frac{\partial}{\partial \widehat{x}} - \frac{\eta_{\widehat{x}} - \eta\eta_{\widehat{x}}}{(h + \eta)^2} \frac{\partial}{\partial \widehat{z}}, \tag{6.14}$$

$$\frac{\partial}{\partial z} = \left(\frac{z}{h + \eta}\right) \frac{\partial}{\partial \widehat{z}}. \tag{6.15}$$

6.3.2 Evaluation of free-surface vertical velocity

In order to evaluate the free-surface vertical velocity in the physical domain with respect to the velocity potential of the mapped domain, we use the expressions for the transformation of the derivatives.

$$
\begin{aligned}
\varphi_z(x) &= \frac{\partial \varphi(x, z = \eta(x,t))}{\partial z} \\
&= \left(\frac{z}{h+\eta}\right) \frac{\partial}{\partial \widehat{z}} \varphi(x, z = \eta(x,t)).
\end{aligned}
$$

By substituting the mapping, $x = \widehat{x}$, $z = \widehat{z}(h+\eta) + \eta$, we get the expression of the free-surface vertical velocity in physical domain, with respect to $\widehat{\varphi}$.

$$
\varphi_z(x) = \left(\widehat{z} + \frac{\eta}{h+\eta}\right) \frac{\partial}{\partial \widehat{z}} \widehat{\varphi}(\widehat{x}, \widehat{z} = 0). \tag{6.16}
$$

After evaluating the free-surface vertical velocity in the physical domain, we use the classical evolution equation (Dommermuth&Yue 1987) to calculate the free-surface η and the free-surface velocity potential φ^S for the next time step.

6.4 Verification of MDSM

The first step of evaluating the results of MDSM is the comparison of the first time step calculation of the free-surface vertical velocity to the results obtained for HOS for the cases A_1, B_1, C_1 and A_2, B_2, C_2. The verification/comparison with respect to the classical high order spectral method was performed for the first time step. It is important to note that for the $B_1$and C_1 cases, we have faced problems because of the value of the wave steepness, $\varepsilon = Ak$. For both thoses cases, the wave steepness exceeded the maximum steepness and the numerical scheme broke down immediately. However, as far as the verification is concerned the results for the first time step of the new numerical method similar with those produced by HOS. The results from the calculation of the free-surface vertical velocity φ_z for the case A_1 is shown in the graph below for HOS and MDSM.

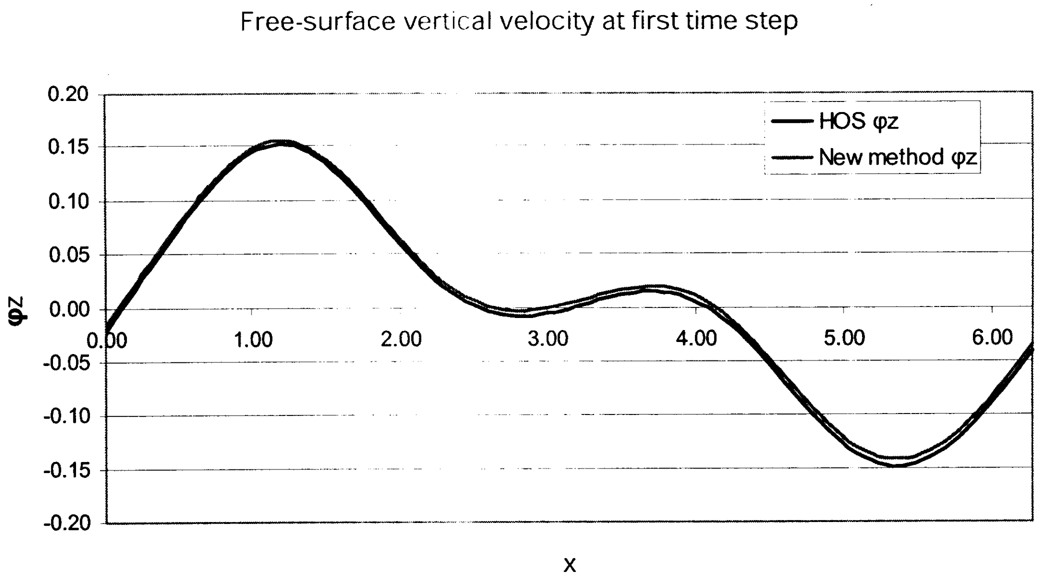

Figure 6-3: Free-surface vertical velocity of the first time step $t = t_1$ for the case A_1

Similar results are given for all cases.

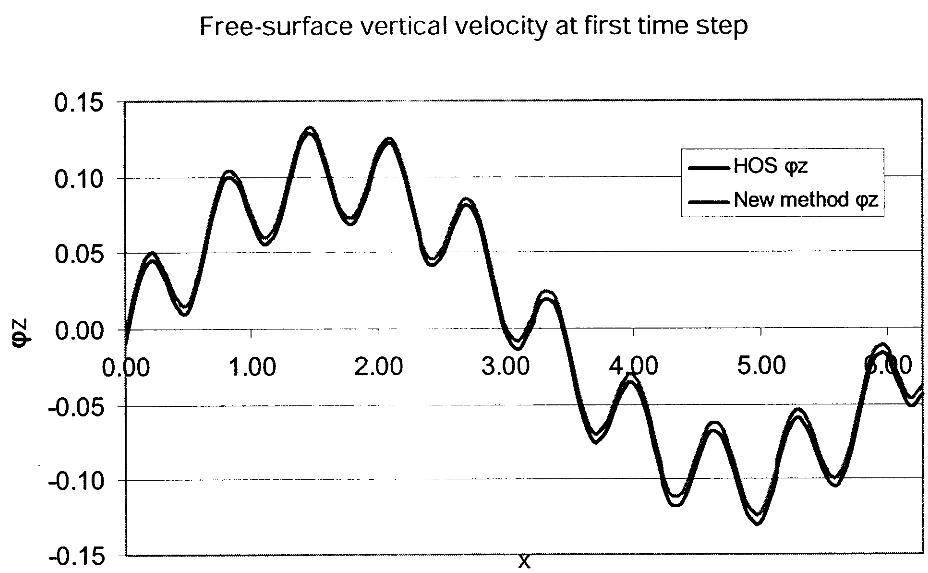

Figure 6-4: Free-surface vertical velocity of the first time step $t = t_1$ for the case A_2

A full set of results for all cases is provided in Appendix D. After having verified the results of MDSM with HOS, we wanted to explore its capabilities in new cases for which the new method was developed.

6.5 New results of MDSM

The new method was developed to treat the problem of long-short wave interactions. Therefore, we focused on cases A_4, B_4 and C_4 for which $\delta = 0.01$. Both HOS and MDSM were simulated for a large number of time steps, namely 400 time steps. For cases A_4 and B_4 results were similar for all time steps. However, for case C_4 HOS was able to provide results only for up to $5T_S = 200$ time steps. MDSM was able to continue the simulation further on and the results on the 198th time step for HOS and MDSM are shown in the following figure.

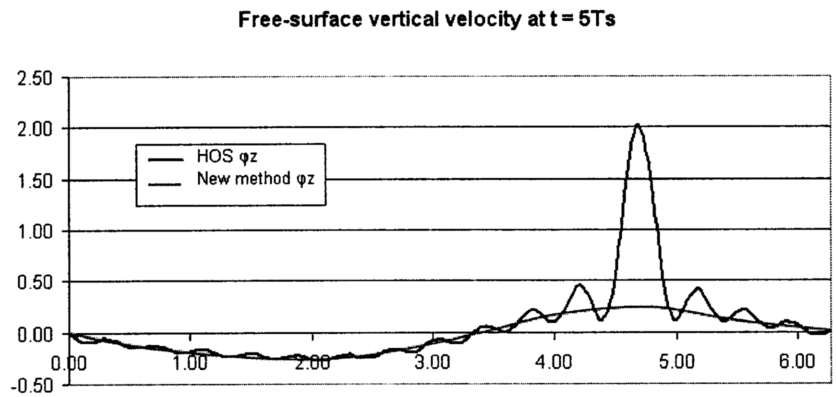

Figure 6-5: Comparison of HOS and MDSM calculation of φ_z for case C_4 at $t = 5T_S$

The above result vendicates the new method and shows its great potential for extending the method for higher orders of nonlinearity.

6.6 Discussion

This method is very promising, however, several issues need further study. More specifically, we have identified two

- The implementation of general boundary conditions needs special treatments
- The calculation of the free-surface vertical velocity with respect to the mapped-domain velocity potential induces new frequencies that may cause for higher values of M convergence issues

6.6.1 General Boundary Conditions

The issue of general boundary conditions could not fully addressed. The case of finite depth was resolved and the results were tested for a number of different initial conditions. However, the generalization in the deep water case was not treated due to problems of matching the boundary conditions between the two different fluid domains. The use of Chebyshev polynomials, however provided promising results near the lower boundary that needs further investigation. The solution of the general problem of deep water can be addressed by the joint solution of lower and upper fluid domains.

6.6.2 Free-surface vertical velocity transformation

The transformation used for the investigation of the problem of long short wave interactions is nonlinear and because of that several problems emerged. The evaluation of the free-surface vertical velocity in the physical domain could not be fully addressed. Instabilities caused the introduction of non-physical frequencies after several steps of time integration. In order to overcome these convergence issues one method that is proposed is to solve the problem fully in the mapped domain. This involves the implementation of the time integration in the mapped domain using the transformed kinematic and dynamic boundary conditions to produce the free-surface elevation and free-surface velocity potential in the mapped domain. The results can then be transformed back to the physical domain using the inverse mapping.

6.7 Future Work

This analysis included a number of different values of ε and δ and was proven to work efficiently for all case with $\varepsilon < \varepsilon_{\text{max}}$. All calculations included terms for up to second order, $M = 2$. Also, analytical results indicated that the generalization of the scheme for $M > 2$ is theoretically guaranteed. There is a vast number of new applications to which this work could evolve. These paths for future work are indicated below:

- Treatment of the general $M-$th nonlinear order of the problem in the mapped domain
- Further study of the nonlinear interactions of multiple waves of different length scales,

$N = O(10)$

- Introduction of capillary effects for the case of very short wave modes

- Investigating the solution of the total problem in the mapped domain using the mapped evolution equations for $\widehat{\varphi}^S$ and $\widehat{\eta}$

- Generalization of the methodology to the 3D case

- Investigation of the general problem of broadband spectrum application for a realistic number of waves of different length scales, $N = 50$

One major application of this specific work is directly related to the reliable interpretation of data gathered by remote sensing techniques. The study of the problem of NWLSI is essential in order to gain understanding of the wave information contained in data gathered by those type of techniques. The current investigation is the first step of the solution of the general 3D, broadband problem of nonlinear interactions for the phase-resolved prediction of large scale wave fields.

Appendix A

Free-surface boundary conditions

In this appendix, we compute in detail the boundary conditions for the free-surface $z = \eta(x,t)$ using Zakharov's formulation introduced in 1968 using the free-surface velocity potential. The boundary conditions are the kinematic boundary condition given by

$$\frac{\partial \eta(x,t)}{\partial t} + \nabla_x \phi(x,z,t) \cdot \nabla_x \eta(x,t) = \frac{\partial \phi(x,z,t)}{\partial z}, \qquad \text{at } z = \eta(x,t) \tag{A.1}$$

and the dynamic boundary condition

$$\frac{\partial \phi(x,z,t)}{\partial t} + \frac{1}{2} \nabla \phi(x,z,t) \cdot \nabla \phi(x,z,t) + gz = 0, \qquad \text{at } z = \eta(x,t)\,. \tag{A.2}$$

using the free-surface velocity potential $\phi^S(x,t) = \phi(x, z = \eta(x,t), t)$ and $x = (x,y)$ when we are working in the 3D case.

The free-surface velocity potential is given by $\phi^S(x,t) = \phi(x, z = \eta(x,t), t)$. Therefore, we can compute the derivatives of ϕ^S with respect to ϕ.

$$\begin{aligned}
\frac{\partial}{\partial t}\left[\phi^S(x,t)\right] &= \frac{\partial}{\partial t}\left[\phi(x, z = \eta(x,t), t)\right] \\
&= \frac{\partial}{\partial t}\left[\phi(x, z = \eta(x,t), t)\right] + \\
&\quad + \frac{\partial}{\partial z}\left[\phi(x, z = \eta(x,t), t)\right] \cdot \frac{\partial}{\partial t}\left[\eta(x,t)\right] \\
&= \frac{\partial \phi}{\partial t} + \frac{\partial \phi}{\partial z} \cdot \frac{\partial \eta}{\partial t}
\end{aligned}$$

Equivalently,

$$
\begin{aligned}
\frac{\partial}{\partial x}\left[\phi^S(x,t)\right] &= \frac{\partial}{\partial x}\left[\phi\left(x, z=\eta\left(x,t\right),t\right)\right] = \\
&= \frac{\partial}{\partial x}\left[\phi\left(x, z=\eta\left(x,t\right),t\right)\right] + \\
&\quad + \frac{\partial}{\partial z}\left[\phi\left(x, z=\eta\left(x,t\right),t\right)\right] \cdot \frac{\partial}{\partial x}\left[\eta\left(x,t\right)\right] \\
&= \frac{\partial \phi}{\partial x} + \frac{\partial \phi}{\partial z} \cdot \frac{\partial \eta}{\partial x}
\end{aligned}
$$

Therefore, we conclude to the following expressions

$$
\frac{\partial \phi}{\partial t} = \frac{\partial \phi^S}{\partial t} - \frac{\partial \phi}{\partial z} \cdot \frac{\partial \eta}{\partial t}, \tag{A.3}
$$

$$
\frac{\partial \phi}{\partial x} = \frac{\partial \phi^S}{\partial x} - \frac{\partial \phi}{\partial z} \cdot \frac{\partial \eta}{\partial x}. \tag{A.4}
$$

where $\frac{\partial \phi}{\partial z}$ is the free-surface velocity.

Before proceeding to the boundary conditions we need to define several parameters of the problem. The formulation given in (C.1) and (A.2) is in general form, so that it applies to both two-dimensional and three-dimensional problems. To be more specific, in the three-dimensional case, we have

$$
\nabla_x \phi\left(x,y,z,t\right) = \left(\frac{\partial \phi}{\partial x}, \frac{\partial \phi}{\partial y}\right),
$$

$$
\nabla \phi\left(x,y,z,t\right) = \left(\frac{\partial \phi}{\partial x}, \frac{\partial \phi}{\partial y}, \frac{\partial \phi}{\partial y}\right).
$$

So, we then compute the terms

$$
\begin{aligned}
\nabla_x \phi\left(x,y,z,t\right) \cdot \nabla_x \eta\left(x,y,t\right) &= \left(\frac{\partial \phi}{\partial x}, \frac{\partial \phi}{\partial y}\right) \cdot \left(\frac{\partial \eta}{\partial x}, \frac{\partial \eta}{\partial y}\right) \\
&= \frac{\partial \phi}{\partial x} \cdot \frac{\partial \eta}{\partial x} + \frac{\partial \phi}{\partial y} \cdot \frac{\partial \eta}{\partial y}
\end{aligned}
$$

$$\begin{aligned}
\nabla\phi(x,z,t)\cdot\nabla\phi(x,z,t) &= \left(\frac{\partial\phi}{\partial x},\frac{\partial\phi}{\partial y},\frac{\partial\phi}{\partial z}\right)\cdot\left(\frac{\partial\phi}{\partial x},\frac{\partial\phi}{\partial y},\frac{\partial\phi}{\partial z}\right) \\
&= \left(\frac{\partial\phi}{\partial x}\right)^2+\left(\frac{\partial\phi}{\partial y}\right)^2+\left(\frac{\partial\phi}{\partial z}\right)^2
\end{aligned}$$

For the two-dimensional case on the other hand, for the same terms, we have

$$\nabla_x\phi(x,z,t)\cdot\nabla_x\eta(x,y,t)=\frac{\partial\phi}{\partial x}\cdot\frac{\partial\eta}{\partial x}, \tag{A.5}$$

$$\nabla\phi(x,z,t)\cdot\nabla\phi(x,z,t)=\left(\frac{\partial\phi}{\partial x},\frac{\partial\phi}{\partial z}\right)\cdot\left(\frac{\partial\phi}{\partial x},\frac{\partial\phi}{\partial z}\right)=\left(\frac{\partial\phi}{\partial x}\right)^2+\left(\frac{\partial\phi}{\partial z}\right)^2. \tag{A.6}$$

We now need to transform these two equations into equivalent ones using the free-surface velocity potential $\phi^S(x,t)=\phi(x,z=\eta(x,t),t)$. Therefore, we take Eq. (C.1) and by using equations (A.5) and (A.4), we obtain

$$\begin{aligned}
\frac{\partial\eta}{\partial t}+\nabla_x\phi(x,z,t)\cdot\nabla_x\eta(x,t)-\frac{\partial\phi(x,z,t)}{\partial z} &= 0 \\
\frac{\partial\eta}{\partial t}+\frac{\partial\phi}{\partial x}\cdot\frac{\partial\eta}{\partial x}-\frac{\partial\phi}{\partial z} &= 0 \\
\frac{\partial\eta}{\partial t}+\left(\frac{\partial\phi^S}{\partial x}-\frac{\partial\phi}{\partial z}\cdot\frac{\partial\eta}{\partial x}\right)\cdot\frac{\partial\eta}{\partial x}-\frac{\partial\phi}{\partial z} &= 0
\end{aligned}$$

By collecting terms, we obtain

$$\frac{\partial\eta}{\partial t}+\frac{\partial\phi^S}{\partial x}\cdot\frac{\partial\eta}{\partial x}-\frac{\partial\phi}{\partial z}\cdot\left(1+\left(\frac{\partial\eta}{\partial x}\right)^2\right)=0$$

In the same way, equation (A.2) becomes using equations (A.3), (A.6) and (A.4)

$$
\begin{aligned}
&\frac{\partial\phi}{\partial t}+\frac{1}{2}\nabla\phi\left(x,z,t\right)\cdot\nabla\phi\left(x,z,t\right)+gz\\
=\;&\left(\frac{\partial\phi^{S}}{\partial t}-\frac{\partial\phi}{\partial z}\cdot\frac{\partial\eta}{\partial t}\right)+\frac{1}{2}\left(\frac{\partial\phi}{\partial x}\right)^{2}+\left(\frac{\partial\phi}{\partial z}\right)^{2}+gz\\
=\;&\left(\frac{\partial\phi^{S}}{\partial t}-\frac{\partial\phi}{\partial z}\cdot\frac{\partial\eta}{\partial t}\right)+\frac{1}{2}\left(\frac{\partial\phi^{S}}{\partial x}-\frac{\partial\phi}{\partial z}\cdot\frac{\partial\eta}{\partial x}\right)^{2}+\left(\frac{\partial\phi}{\partial z}\right)^{2}+gz\\
=\;&\frac{\partial\phi^{S}}{\partial t}-\frac{\partial\phi}{\partial z}\cdot\frac{\partial\eta}{\partial t}++\frac{1}{2}\left(\left(\frac{\partial\phi^{S}}{\partial x}\right)^{2}+\left(\frac{\partial\phi}{\partial z}\cdot\frac{\partial\eta}{\partial x}\right)^{2}-2\frac{\partial\phi^{S}}{\partial x}\frac{\partial\phi}{\partial z}\cdot\frac{\partial\eta}{\partial x}\right)+\left(\frac{\partial\phi}{\partial z}\right)^{2}+gz
\end{aligned}
$$

$$
\begin{aligned}
\frac{\partial\phi^{S}}{\partial t}\;=\;&\frac{\partial\phi}{\partial z}\cdot\frac{\partial\eta}{\partial t}+\frac{1}{2}\left(\frac{\partial\phi^{S}}{\partial x}\right)^{2}-\frac{1}{2}\left(\frac{\partial\phi}{\partial z}\cdot\frac{\partial\eta}{\partial x}\right)^{2}+\\
&+\frac{\partial\phi^{S}}{\partial x}\frac{\partial\phi}{\partial z}\cdot\frac{\partial\eta}{\partial x}+\left(\frac{\partial\phi}{\partial z}\right)^{2}-gz
\end{aligned}
$$

We now need to substitute $\frac{\partial\zeta}{\partial t}$using equation (A.7), that is.

$$
\frac{\partial\eta}{\partial t}=-\frac{\partial\phi^{S}}{\partial x}\cdot\frac{\partial\eta}{\partial x}+\frac{\partial\phi}{\partial z}\cdot\left(1+\left(\frac{\partial\eta}{\partial x}\right)^{2}\right)
$$

$$
\frac{\partial\phi^{S}}{\partial t}-\frac{\partial\phi}{\partial z}\cdot\left(-\frac{\partial\phi^{S}}{\partial x}\cdot\frac{\partial\eta}{\partial x}+\frac{\partial\phi}{\partial z}\cdot\left(1+\left(\frac{\partial\eta}{\partial x}\right)^{2}\right)\right)+\frac{1}{2}\left(\frac{\partial\phi^{S}}{\partial x}\right)^{2}+
$$

$$
+\frac{1}{2}\left(\frac{\partial\phi}{\partial z}\cdot\frac{\partial\eta}{\partial x}\right)^{2}-\frac{\partial\phi^{S}}{\partial x}\frac{\partial\phi}{\partial z}\cdot\frac{\partial\eta}{\partial x}+\left(\frac{\partial\phi}{\partial z}\right)^{2}+g\eta=0
$$

$$
\frac{\partial\phi^{S}}{\partial t}-\frac{\partial\phi}{\partial z}\cdot\left(-\frac{\partial\phi^{S}}{\partial x}\cdot\frac{\partial\eta}{\partial x}+\frac{\partial\phi}{\partial z}\cdot\left(1+\left(\frac{\partial\eta}{\partial x}\right)^{2}\right)\right)+\frac{1}{2}\left(\frac{\partial\phi^{S}}{\partial x}\right)^{2}
$$

$$
+\frac{1}{2}\left(\frac{\partial\phi}{\partial z}\cdot\frac{\partial\zeta}{\partial x}\right)^{2}-\frac{\partial\phi^{S}}{\partial x}\frac{\partial\phi}{\partial z}\cdot\frac{\partial\zeta}{\partial x}+\left(\frac{\partial\phi}{\partial z}\right)^{2}+g\zeta=0
$$

$$
\frac{\partial\phi^{S}}{\partial t}+\underbrace{\frac{\partial\phi}{\partial z}\cdot\frac{\partial\phi^{S}}{\partial x}\cdot\frac{\partial\eta}{\partial x}}-\left(\frac{\partial\phi}{\partial z}\right)^{2}-\left(\frac{\partial\phi}{\partial z}\right)^{2}\cdot\left(\frac{\partial\eta}{\partial x}\right)^{2}+
$$

$$
+\frac{1}{2}\left(\frac{\partial\phi^{S}}{\partial x}\right)^{2}+\frac{1}{2}\left(\frac{\partial\phi}{\partial z}\cdot\frac{\partial\eta}{\partial x}\right)^{2}-\underbrace{\frac{\partial\phi^{S}}{\partial x}\cdot\frac{\partial\phi}{\partial z}\cdot\frac{\partial\eta}{\partial x}}+\left(\frac{\partial\phi}{\partial z}\right)^{2}+g\eta=0
$$

$$\frac{\partial \phi^S}{\partial t} - \left(\frac{\partial \phi}{\partial z}\right)^2 - \left(\frac{\partial \phi}{\partial z}\right)^2 \cdot \left(\frac{\partial \eta}{\partial x}\right)^2 + \frac{1}{2}\left(\frac{\partial \phi^S}{\partial x}\right)^2 + \frac{1}{2}\left(\frac{\partial \phi}{\partial z} \cdot \frac{\partial \eta}{\partial x}\right)^2 + \left(\frac{\partial \phi}{\partial z}\right)^2 + g\eta = 0$$

And finally, we get

$$\frac{\partial \phi^S}{\partial t} + \frac{1}{2}\left(\frac{\partial \phi^S}{\partial x}\right)^2 - \frac{1}{2}\left(1 + \left(\frac{\partial \eta}{\partial x}\right)^2\right)\left(\frac{\partial \phi}{\partial z}\right)^2 + g\eta = 0$$

To sum up the boundary conditions are given by the kinematic boundary condition, i.e.

$$\frac{\partial \eta}{\partial t} + \frac{\partial \phi^S}{\partial x} \cdot \frac{\partial \eta}{\partial x} - \frac{\partial \phi}{\partial z} \cdot \left(1 + \left(\frac{\partial \eta}{\partial x}\right)^2\right) = 0, \qquad \text{at } z = \eta\left(x, t\right) \tag{A.7}$$

and the dynamic boundary condition

$$\frac{\partial \phi^S}{\partial t} + \frac{1}{2}\left(\frac{\partial \phi^S}{\partial x}\right)^2 - \frac{1}{2}\left(1 + \left(\frac{\partial \eta}{\partial x}\right)^2\right)\left(\frac{\partial \phi}{\partial z}\right)^2 + g\eta + \frac{p}{\rho} = 0 \quad \text{at } z = \eta\left(x, t\right) \tag{A.8}$$

Appendix B

Transformation of variables

Suppose we define the following general transformation of variables

$$\begin{aligned} x &= f\left(\widehat{x},\widehat{z}\right) \\ z &= g\left(\widehat{x},\widehat{z}\right). \end{aligned}$$

Accordingly, let us assume that the inverse transformation also exists

$$\begin{aligned} \widehat{x} &= f^{-1}\left(x,z\right) = h\left(x,z\right) \\ \widehat{z} &= g^{-1}\left(\widehat{x},\widehat{z}\right) = k\left(x,z\right). \end{aligned}$$

The first order derivatives are transformed using chain rule

$$\frac{\partial}{\partial x} = \frac{\partial}{\partial \widehat{x}}\frac{\partial \widehat{x}}{\partial x} + \frac{\partial}{\partial \widehat{z}}\frac{\partial \widehat{z}}{\partial x},$$

$$\frac{\partial}{\partial z} = \frac{\partial}{\partial \widehat{x}}\frac{\partial \widehat{x}}{\partial z} + \frac{\partial}{\partial \widehat{z}}\frac{\partial \widehat{z}}{\partial z}.$$

This leads to

$$\frac{\partial}{\partial x} = \frac{\partial}{\partial \widehat{x}}\frac{\partial h\left(x,z\right)}{\partial x} + \frac{\partial}{\partial \widehat{z}}\frac{\partial k\left(x,z\right)}{\partial x},$$

$$\frac{\partial}{\partial z}=\frac{\partial}{\partial \widehat{x}}\frac{\partial h\left(x,z\right)}{\partial z}+\frac{\partial}{\partial \widehat{z}}\frac{\partial k\left(x,z\right)}{\partial z}.$$

The second order derivatives are transformed accordingly

$$\frac{\partial^2}{\partial x^2}=\frac{\partial}{\partial x}\left[\frac{\partial}{\partial \widehat{x}}\frac{\partial \widehat{x}}{\partial x}+\frac{\partial}{\partial \widehat{z}}\frac{\partial \widehat{z}}{\partial x}\right],$$

$$\frac{\partial^2}{\partial z^2}=\frac{\partial}{\partial z}\left[\frac{\partial}{\partial \widehat{x}}\frac{\partial \widehat{x}}{\partial z}+\frac{\partial}{\partial \widehat{z}}\frac{\partial \widehat{z}}{\partial z}\right].$$

We proceed with the calculations for each second order derivative

$$\begin{aligned}
\frac{\partial^2}{\partial x^2} &= \frac{\partial}{\partial x}\left[\frac{\partial}{\partial \widehat{x}}\frac{\partial \widehat{x}}{\partial x}+\frac{\partial}{\partial \widehat{z}}\frac{\partial \widehat{z}}{\partial x}\right]\\
&= \frac{\partial}{\partial x}\left(\frac{\partial}{\partial \widehat{x}}\frac{\partial \widehat{x}}{\partial x}\right)+\frac{\partial}{\partial x}\left(\frac{\partial}{\partial \widehat{z}}\frac{\partial \widehat{z}}{\partial x}\right)\\
&= \frac{\partial^2}{\partial x\partial \widehat{x}}\frac{\partial \widehat{x}}{\partial x}+\frac{\partial}{\partial \widehat{x}}\frac{\partial^2 \widehat{x}}{\partial x^2}+\frac{\partial^2}{\partial x\partial \widehat{z}}\frac{\partial \widehat{z}}{\partial x}+\frac{\partial}{\partial \widehat{z}}\frac{\partial^2 \widehat{z}}{\partial x^2}\\
&= \frac{\partial}{\partial \widehat{x}}\left[\frac{\partial}{\partial \widehat{x}}\frac{\partial \widehat{x}}{\partial x}+\frac{\partial}{\partial \widehat{z}}\frac{\partial \widehat{z}}{\partial x}\right]\frac{\partial \widehat{x}}{\partial x}+\frac{\partial}{\partial \widehat{x}}\frac{\partial^2 \widehat{x}}{\partial x^2}+\\
&\quad +\frac{\partial}{\partial \widehat{z}}\left[\frac{\partial}{\partial \widehat{x}}\frac{\partial \widehat{x}}{\partial x}+\frac{\partial}{\partial \widehat{z}}\frac{\partial \widehat{z}}{\partial x}\right]\frac{\partial \widehat{z}}{\partial x}+\frac{\partial}{\partial \widehat{z}}\frac{\partial^2 \widehat{z}}{\partial x^2}\\
&= \frac{\partial^2}{\partial \widehat{x}^2}\left(\frac{\partial \widehat{x}}{\partial x}\right)^2+\frac{\partial^2}{\partial \widehat{z}\partial \widehat{x}}\frac{\partial \widehat{z}}{\partial x}\frac{\partial \widehat{x}}{\partial x}+\frac{\partial}{\partial \widehat{x}}\frac{\partial^2 \widehat{x}}{\partial x^2}+\\
&\quad +\frac{\partial^2}{\partial \widehat{z}\partial \widehat{x}}\frac{\partial \widehat{x}}{\partial x}\frac{\partial \widehat{z}}{\partial x}+\frac{\partial^2}{\partial \widehat{z}^2}\left(\frac{\partial \widehat{z}}{\partial x}\right)^2+\frac{\partial}{\partial \widehat{z}}\frac{\partial^2 \widehat{z}}{\partial x^2}\\
&= \frac{\partial^2}{\partial \widehat{x}^2}\left(\frac{\partial \widehat{x}}{\partial x}\right)^2+\frac{\partial^2}{\partial \widehat{z}^2}\left(\frac{\partial \widehat{z}}{\partial x}\right)^2+2\frac{\partial^2}{\partial \widehat{z}\partial \widehat{x}}\frac{\partial \widehat{z}}{\partial x}\frac{\partial \widehat{x}}{\partial x}+\\
&\quad +2\frac{\partial^2}{\partial \widehat{z}\partial \widehat{x}}\frac{\partial \widehat{z}}{\partial x}\frac{\partial \widehat{x}}{\partial x}+\frac{\partial}{\partial \widehat{x}}\frac{\partial^2 \widehat{x}}{\partial x^2}+\frac{\partial}{\partial \widehat{z}}\frac{\partial^2 \widehat{z}}{\partial x^2}
\end{aligned}$$

In the same way we calculate the second derivative with respect to z

$$
\begin{aligned}
\frac{\partial^2}{\partial z^2} &= \frac{\partial}{\partial z}\left[\frac{\partial}{\partial \widehat{x}}\frac{\partial \widehat{x}}{\partial z}+\frac{\partial}{\partial \widehat{z}}\frac{\partial \widehat{z}}{\partial z}\right] \\
&= \frac{\partial}{\partial z}\left(\frac{\partial}{\partial \widehat{x}}\frac{\partial \widehat{x}}{\partial z}\right)+\frac{\partial}{\partial z}\left(\frac{\partial}{\partial \widehat{z}}\frac{\partial \widehat{z}}{\partial z}\right) \\
&= \frac{\partial^2}{\partial z\partial \widehat{x}}\frac{\partial \widehat{x}}{\partial z}+\frac{\partial}{\partial \widehat{x}}\frac{\partial^2 \widehat{x}}{\partial z^2}+\frac{\partial^2}{\partial z\partial \widehat{z}}\frac{\partial \widehat{z}}{\partial z}+\frac{\partial}{\partial \widehat{z}}\frac{\partial^2 \widehat{z}}{\partial z^2} \\
&= \frac{\partial}{\partial \widehat{x}}\left[\frac{\partial}{\partial \widehat{x}}\frac{\partial \widehat{x}}{\partial z}+\frac{\partial}{\partial \widehat{z}}\frac{\partial \widehat{z}}{\partial z}\right]\frac{\partial \widehat{x}}{\partial z}+\frac{\partial}{\partial \widehat{x}}\frac{\partial^2 \widehat{x}}{\partial z^2}+ \\
&\quad +\frac{\partial}{\partial \widehat{z}}\left[\frac{\partial}{\partial \widehat{x}}\frac{\partial \widehat{x}}{\partial z}+\frac{\partial}{\partial \widehat{z}}\frac{\partial \widehat{z}}{\partial z}\right]\frac{\partial \widehat{z}}{\partial z}+\frac{\partial}{\partial \widehat{z}}\frac{\partial^2 \widehat{z}}{\partial z^2} \\
&= \frac{\partial^2}{\partial \widehat{x}^2}\left(\frac{\partial \widehat{x}}{\partial z}\right)^2+\frac{\partial^2}{\partial \widehat{z}\partial \widehat{x}}\frac{\partial \widehat{z}}{\partial z}\frac{\partial \widehat{x}}{\partial z}+\frac{\partial}{\partial \widehat{x}}\frac{\partial^2 \widehat{x}}{\partial z^2}+ \\
&\quad +\frac{\partial^2}{\partial \widehat{z}\partial \widehat{x}}\frac{\partial \widehat{x}}{\partial z}\frac{\partial \widehat{z}}{\partial z}+\frac{\partial^2}{\partial \widehat{z}^2}\left(\frac{\partial \widehat{z}}{\partial z}\right)^2+\frac{\partial}{\partial \widehat{z}}\frac{\partial^2 \widehat{z}}{\partial z^2} \\
&= \frac{\partial^2}{\partial \widehat{x}^2}\left(\frac{\partial \widehat{x}}{\partial z}\right)^2+\frac{\partial^2}{\partial \widehat{z}^2}\left(\frac{\partial \widehat{z}}{\partial z}\right)^2+2\frac{\partial^2}{\partial \widehat{z}\partial \widehat{x}}\frac{\partial \widehat{z}}{\partial z}\frac{\partial \widehat{x}}{\partial z}+ \\
&\quad +\frac{\partial}{\partial \widehat{x}}\frac{\partial^2 \widehat{x}}{\partial z^2}+\frac{\partial}{\partial \widehat{z}}\frac{\partial^2 \widehat{z}}{\partial z^2}
\end{aligned}
$$

This leads to

$$
\begin{aligned}
\frac{\partial^2}{\partial x^2} &= \frac{\partial^2}{\partial \widehat{x}^2}\left(\frac{\partial h(x,z)}{\partial x}\right)^2+\frac{\partial^2}{\partial \widehat{z}^2}\left(\frac{\partial k(x,z)}{\partial x}\right)^2+ \\
&\quad +2\frac{\partial^2}{\partial \widehat{z}\partial \widehat{x}}\frac{\partial k(x,z)}{\partial x}\frac{\partial h(x,z)}{\partial x}+\frac{\partial}{\partial \widehat{x}}\frac{\partial^2 h(x,z)}{\partial x^2}+\frac{\partial}{\partial \widehat{z}}\frac{\partial^2 k(x,z)}{\partial x^2},
\end{aligned}
$$

$$
\begin{aligned}
\frac{\partial^2}{\partial z^2} &= \frac{\partial^2}{\partial \widehat{x}^2}\left(\frac{\partial h(x,z)}{\partial z}\right)^2+\frac{\partial^2}{\partial \widehat{z}^2}\left(\frac{\partial k(x,z)}{\partial z}\right)^2+ \\
&\quad +2\frac{\partial^2}{\partial \widehat{z}\partial \widehat{x}}\frac{\partial k(x,z)}{\partial z}\frac{\partial h(x,z)}{\partial z}+\frac{\partial}{\partial \widehat{x}}\frac{\partial^2 h(x,z)}{\partial z^2}+\frac{\partial}{\partial \widehat{z}}\frac{\partial^2 k(x,z)}{\partial z^2}.
\end{aligned}
$$

Therefore, Laplace's equation is transformed as follows

$$
\begin{aligned}
\nabla^2 &= \frac{\partial^2}{\partial x^2}+\frac{\partial^2}{\partial z^2}\\
&= \frac{\partial^2}{\partial \widehat{x}^2}\left(\frac{\partial h\left(x,z\right)}{\partial x}\right)^2+\frac{\partial^2}{\partial \widehat{z}^2}\left(\frac{\partial k\left(x,z\right)}{\partial x}\right)^2+\\
&+2\frac{\partial^2}{\partial \widehat{z}\partial \widehat{x}}\frac{\partial k\left(x,z\right)}{\partial x}\frac{\partial h\left(x,z\right)}{\partial x}+\frac{\partial}{\partial \widehat{x}}\frac{\partial^2 h\left(x,z\right)}{\partial x^2}+\frac{\partial}{\partial \widehat{z}}\frac{\partial^2 k\left(x,z\right)}{\partial x^2}+\\
&+\frac{\partial^2}{\partial \widehat{x}^2}\left(\frac{\partial h\left(x,z\right)}{\partial z}\right)^2+\frac{\partial^2}{\partial \widehat{z}^2}\left(\frac{\partial k\left(x,z\right)}{\partial z}\right)^2+\\
&+2\frac{\partial^2}{\partial \widehat{z}\partial \widehat{x}}\frac{\partial k\left(x,z\right)}{\partial z}\frac{\partial h\left(x,z\right)}{\partial z}+\frac{\partial}{\partial \widehat{x}}\frac{\partial^2 h\left(x,z\right)}{\partial z^2}+\frac{\partial}{\partial \widehat{z}}\frac{\partial^2 k\left(x,z\right)}{\partial z^2}.
\end{aligned}
$$

We now move on to the specific change of variables that we employ for our analysis, given by

$$
\begin{aligned}
x &= \widehat{x}=f\left(\widehat{x},\widehat{z}\right),\\
z &= \widehat{z}\left(h+\eta\right)+\eta=g\left(\widehat{x},\widehat{z}\right).
\end{aligned}
$$

Accordingly, the inverse transformation is given by

$$
\begin{aligned}
\widehat{x} &= x=h\left(x,z\right)\\
\widehat{z} &= \frac{z-\eta}{\left(h+\eta\right)}=k\left(x,z\right).
\end{aligned}
$$

The first order derivatives are transformed using chain rule are

$$
\begin{aligned}
\frac{\partial}{\partial x} &= \frac{\partial}{\partial \widehat{x}}-\frac{\partial}{\partial \widehat{z}}\frac{\eta_{\widehat{x}}-\eta\eta_{\widehat{x}}}{\left(h+\eta\right)^2},\\
\frac{\partial}{\partial z} &= \frac{\partial}{\partial \widehat{z}}\left(\frac{z}{h+\eta}\right).
\end{aligned}
$$

The Laplace equation therefore is given by the following expression

$$
\begin{aligned}
\nabla^2 &= \frac{\partial^2}{\partial\widehat{x}^2}\left(\frac{\partial h(x,z)}{\partial x}\right)^2+\frac{\partial^2}{\partial\widehat{z}^2}\left(\frac{\partial k(x,z)}{\partial x}\right)^2+2\frac{\partial^2}{\partial\widehat{z}\partial\widehat{x}}\frac{\partial k(x,z)}{\partial x}\frac{\partial h(x,z)}{\partial x} \\
&\quad+\frac{\partial}{\partial\widehat{x}}\frac{\partial^2 h(x,z)}{\partial x^2}+\frac{\partial}{\partial\widehat{z}}\frac{\partial^2 k(x,z)}{\partial x^2}+\frac{\partial^2}{\partial\widehat{x}^2}\left(\frac{\partial h(x,z)}{\partial z}\right)^2+\frac{\partial^2}{\partial\widehat{z}^2}\left(\frac{\partial k(x,z)}{\partial z}\right)^2+ \\
&\quad+2\frac{\partial^2}{\partial\widehat{z}\partial\widehat{x}}\frac{\partial k(x,z)}{\partial z}\frac{\partial h(x,z)}{\partial z}+\frac{\partial}{\partial\widehat{x}}\frac{\partial^2 h(x,z)}{\partial z^2}+\frac{\partial}{\partial\widehat{z}}\frac{\partial^2 k(x,z)}{\partial z^2}= \\
&= \frac{\partial^2}{\partial\widehat{x}^2}+\frac{\partial^2}{\partial\widehat{z}^2}\left[\left(\frac{\eta_x(h+z)}{h+\eta}\right)^2+\left(\frac{1}{h+\eta}\right)^2\right]+ \\
&\quad-2\frac{\partial^2}{\partial\widehat{z}\partial\widehat{x}}\frac{\eta_x(h+z)}{(h+\eta)^2}+\frac{\partial}{\partial\widehat{z}}\frac{-\eta_{xx}(h+\eta)+2\eta_x^2(h+z)(h+\eta)}{(h+\eta)^4}
\end{aligned}
$$

Appendix C

Mode-Coupled Model

In the case of an homogeneous, inviscid and incompressible, 3D fluid that lies under a free surface in deep water regime the important variables that characterize the problem are given by:

- Free-surface: $\eta(x,t) = \frac{1}{2}\sum_k e_k^{ikx}\eta(t) + c.c.$

  Velocity Potential: $\phi(x,z,t) = \frac{1}{2}\sum_k e^{ikx}e^{\kappa z}\phi_k(t) + c.c.$

where $k = (k_x + k_y)$, $e^{ikx} = e^{i(k_x x + k_y y)}$ and κ is the magnitude of the wave vector k defined by $\kappa = \left(k_x^2 + k_y^2\right)^{1/2}$.

Note: The above expressions are equivalently defined for the 2D case where $k = (k_x)$, $e^{ikx} = e^{i(k_x x)}$ and $\kappa = k$. As from now we will be working in the 2D case.

The equations of motion for the case of an irrotational, incompressible, inviscid free-surface $\eta\,(x,t)$, are given by

$$\frac{\partial\eta\,(x,t)}{\partial t} + \nabla_x\phi\,(x,z,t)\cdot\nabla_x\eta\,(x,t) = \frac{\partial\phi\,(x,z,t)}{\partial z}, \tag{C.1}$$

$$\frac{\partial\phi\,(x,z,t)}{\partial t} + \frac{1}{2}\nabla\phi\,(x,z,t)\cdot\nabla\phi\,(x,z,t) + gz = 0. \tag{C.2}$$

Inside the fluid domain, due to the condition of incompressibility, Laplace's equation holds for $\phi(x, z, t)$, i.e.

$$\nabla^2 \phi(x, z, t) = 0, \tag{C.3}$$

which is the reason to justify expressions for $\eta(x, t)$ and $\phi(x, z, t)$ respectively given earlier.

Using the free-surface velocity potential $\phi^S(x, t) = \phi(x, z = \eta(x, t), t)$ the equations of motion become

$$\frac{\partial \eta}{\partial t} + \nabla_x \phi^S \cdot \nabla_x \eta = (1 + \nabla_x \eta \cdot \nabla_x \eta) \frac{\partial \phi}{\partial z}, \tag{C.4}$$

$$\frac{\partial \phi^S}{\partial t} + \frac{1}{2} \nabla_x \phi^S \cdot \nabla_x \phi^S + gz = \frac{1}{2} \left(1 + \nabla_x \eta \cdot \nabla_x \eta \frac{\partial \phi}{\partial z}\right), \tag{C.5}$$

where $\nabla_x \cdot$ is the gradient in the horizontal direction x, i.e.$\nabla_x \cdot = \left(\frac{\partial \cdot}{\partial x}, \frac{\partial \cdot}{\partial y}\right)$ in the 3D case, $\nabla_x \cdot = \left(\frac{\partial \cdot}{\partial x}\right)$ in the 2D and $\frac{\partial \phi(x, z=\eta, t)}{\partial z}$ is the free-surface velocity at each point x and at each time t. An elaborate description of the derivation of equations (C.5) and (C.4) in the 2D case is presented in Appendix A.

On the free surface the velocity potential is given by $\phi^S(x, t) = \phi(x, z = \eta(x, t), t) = \frac{1}{2} \sum_k e^{ikx} e^{k\zeta} \phi_k(t) + c.c.$. Therefore, the free-surface velocity potential becomes an exponential function of η. In order to avoid that we use a Taylor expansion series to approximate the term $e^{k\eta}$ for every mode different mode k.

After the Taylor expansion of $\phi^S(x, t)$ around the mean free-surface we have

$$\phi^S(x, t) = \frac{1}{2} \sum_k e^{ikx} \left(\sum_{n=0}^{\infty} \frac{(k\eta)^n}{n!} \right) \phi_k(t) + c.c. \tag{C.6}$$

By rearranging the limits, we get

$$\phi^S(x, t) = \frac{1}{2} \sum_{n=0}^{\infty} \frac{(\eta)^n}{n!} \left(\sum_k e^{ikx} k^n \phi_k(t) \right) + c.c. \tag{C.7}$$

Assume now we have only two different waves, a long a_L, k_L and a short a_S, k_S. Then, Eq. (C.6) becomes

$$\phi^S(x,t) = \sin(k_L x)\left(\sum_{n=0}^{\infty}\frac{(k_L\ \eta)^n}{n!}\right)\phi_{k_L}(t) + \tag{C.8}$$

$$+\sin(k_S x)\left(\sum_{n=0}^{\infty}\frac{(k_S\ \eta)^n}{n!}\right)\phi_{k_S}(t). \tag{C.9}$$

Therefore, for Eq. (C.8) we obtain

$$\phi^S(x,t) = \sin(k_L x)\left(\sum_{n=0}^{\infty}\frac{(k_L(\eta_L+\eta_S))^n}{n!}\right)\phi_{k_L}(t) + \tag{C.10}$$

$$+\sin(k_S x)\left(\sum_{n=0}^{\infty}\frac{(k_S\ (\eta_L+\eta_S))^n}{n!}\right)\phi_{k_S}(t) \tag{C.11}$$

with

$$\eta(x,t) = \eta_L(x,t) + \eta_S(x,t) = \cos(k_L x)\,\eta_{k_L}(t) + \cos(k_S x)\,\eta_{k_S}(t)$$

where η_L is proportional to a_L and η_S is proportional to a_S.

Problem: The expression given in (C.10) does not converge rapidly because the second term contains series of the form $\sum_{n=0}^{\infty}\frac{(k_S\ a_L)^n}{n!}$, which for the case of long short wave interaction represents a large number. To be more specific, let's say that $k_L = 0.01\ cm^{-1}$, $a_L = 10\ cm$ and $k_S = 0.1\ cm^{-1}$, $a_S = 1\ cm$. Therefore, in equation (C.10) the series $\sum_{n=0}^{\infty}\frac{(k_S\ a_L)^n}{n!} = \sum_{n=0}^{\infty}\frac{(1)^n}{n!}$ converges very slowly. Therefore some claim that "*Modal-expansion models are only useful for the prediction of narrow wave spectra evolution*".

We now return in the expression of the velocity potential

$$\phi^S(x,t) = \frac{1}{2}\sum_{n=0}^{\infty}\frac{\eta^n}{n!}k^n\phi_0(x,t) + c.c. \tag{C.12}$$

where $k^n\phi_0(x,t) = \sum_k k^n e^{ikx}\phi_0^k(t)$.

Equivalently we have that the vertical velocity of the free-surface is given by

$$\begin{aligned} W(x,t) &= \frac{\partial \phi}{\partial z} \text{ at } z = \eta(x,t) = \\ &= \frac{1}{2}\sum_{n=0}^{\infty} \frac{\eta^n}{n!} k^{n+1} \phi_0(x,t) + c.c. \end{aligned} \tag{C.13}$$

where $k^{n+1}\phi_0(x,t) = \sum_k k^{n+1} e^{ikx} \phi_0^k(t)$.

Following West (1988) analysis we write $\phi^S(x,t)$ and $W(x,t)$ in terms of operators. To be more specific, starting from equations (C.12) and (C.13) we have

$$\phi^S(x,t) = O(x,t)\,\phi_0(x,t). \tag{C.14}$$

The operator $O(x,t)\cdot \; = \sum_{n=0}^{\infty} \frac{\zeta^n}{n!} k^n \cdot$ represents the projection of the velocity potential defined on the $z = 0$ reference plane onto the free-surface. The inverse operator $O^{-1}(x,t)$ represents the projection of the velocity potential from the free-surface back onto the reference plane, i.e.

$$\phi_0(x,t) = O^{-1}(x,t)\,\phi^S(x,t). \tag{C.15}$$

We know that

$$O(x,t)\cdot \; = \sum_{n=0}^{\infty} O_n \cdot \; = O_0 + O_1 + O_2 + ... \tag{C.16}$$

where $O_0 = 1$.

In order to compute the inverse operator, we work as follows

$$\begin{aligned} O^{-1}(x,t)\cdot &= (O_0 + O_1 + O_2 + ...)\cdot \; = \\ &= (1 + (O_1 + O_2 + ...))\cdot \end{aligned}$$

By using binomial series given by

$$(1+x)^{-1} = 1 - x + x^2 - x^3 + ... \tag{C.17}$$

we obtain for the inverse of $O\,(x,t)$

$$O^{-1}\,(x,t)\cdot\ =\left(1-(O_1+O_2)+(O_1+O_2)^2-(O_1+O_2)^3+...\right)\cdot \tag{C.18}$$

Therefore, the expression for the free-surface vertical velocity that is initially given by

$$W\,(x,t)=Q\,(x,t)\,\phi_0(x,t) \tag{C.19}$$

can be transformed using (C.15) into

$$W\,(x,t)=Q\,(x,t)\,O^{-1}\,(x,t)\,\phi^S(x,t), \tag{C.20}$$

where $Q\,(x,t)\cdot\ =\sum_{n=0}^{\infty}\frac{\eta^n}{n!}k^{n+1}\cdot$.

Knowing the expression of $O^{-1}\,(x,t)$ and $Q\,(x,t)$ in terms of O_n and Q_n, that is

$$Q\,(x,t)\cdot\ =\sum_{n=0}^{\infty}Q_n\cdot\ =(Q_0+Q_1+Q_2+...)\cdot$$

$$O^{-1}\,(x,t)\cdot\ =\left(1-(O_1+O_2)+(O_1+O_2)^2-(O_1+O_2)^3+...\right)\cdot$$

the vertical velocity becomes

$$\begin{aligned} W\,(x,t) &= Q\,(x,t)\,O^{-1}\,(x,t)\,\phi^S(x,t) \\ &= (Q_0+Q_1+Q_2+...)\left(1-(O_1+O_2)+(O_1+O_2)^2-(O_1+O_2)^3+...\right)\phi^S(x,t) \end{aligned}$$

Also, we have that $W\,(x,t)$ is represented as a series, i.e.

$$W\,(x,t)=\sum_{n=0}^{\infty}W_n=W_0+W_1+W_2+...$$

We now need to represent the n-th terms of the vertical velocity of the free-surface, that is W_n in terms of O_n and Q_n.

$$
\begin{aligned}
W_0 &= Q_0 \phi^S(x,t) \\
W_1 &= (Q_1 - Q_0 O_1)\, \phi^S(x,t) \\
W_2 &= \left(Q_2 - Q_1 O_1 - Q_0 O_1^2\right) \phi^S(x,t) \\
W_3 &= \left(Q_2 O_1 - Q_1 O_2 - Q_1 O_1^2 - Q_0 O_1 O_2 - Q_0 O_2 O_1\right) \phi^S(x,t) \\
\dots &= \dots \\
W_n &= (\textit{Milder JFM } 1990)
\end{aligned}
$$

We need to prove that all terms of W are proportional to $\varepsilon = a_L k_L = a_S k_S$.

Appendix D

Cases results

This section contains the results of the simulation of the new Mapped-Domain Spectral Method (MDSM) for the case of two interacting waves. As it was originally described in Chapter 6, we will set up a number of different test cases based on two non-dimensional parameters. The first parameter is defined to be the steepness of the interacting waves $\varepsilon = kA$. The second parameters is given by $\delta = \lambda_S / \lambda_L$. The following table gives the case numbering according to the values of ε and δ. This table was introduced in Chapter 6 and is presented here also for convenience.

ε \ δ	0.5	0.1	0.01	1
0.1	A_1	A_2	A_3	A_4
0.2	B_1	B_2	B_3	B_4
0.3	C_1	C_2	C_3	C_4

Figure D1 Test cases classification table

The following figures provide the calculated free-surface vertical velocity for the first time step, using both HOS and MDSM. This section provided the first proof of the reliability of new method for obtaining φ_z using the new, mapped-domain approach. In order to benchmark the method, we simulated the interaction of two waves for different values of ε and δ. The results of the first time step calculation of the free-surface vertical velocity using both the HOS method and MDSM are given for all cases presented in Fig. D1. After this preliminary analysis, we proceeded in long time simulations. The results of this analysis are presented in Chapter 6.

Case A1

Wave characteristics:

- Long wave $A_L = 0.1$, $k_L = 1$
- Short wave $A_S = 0.05$, $k_S = 2$

Study Parameters:

- Steepness $\varepsilon = A_S k_S = A_L k_L = 0.1$
- Length scale $\delta = \lambda_S / \lambda_L = 0.5$

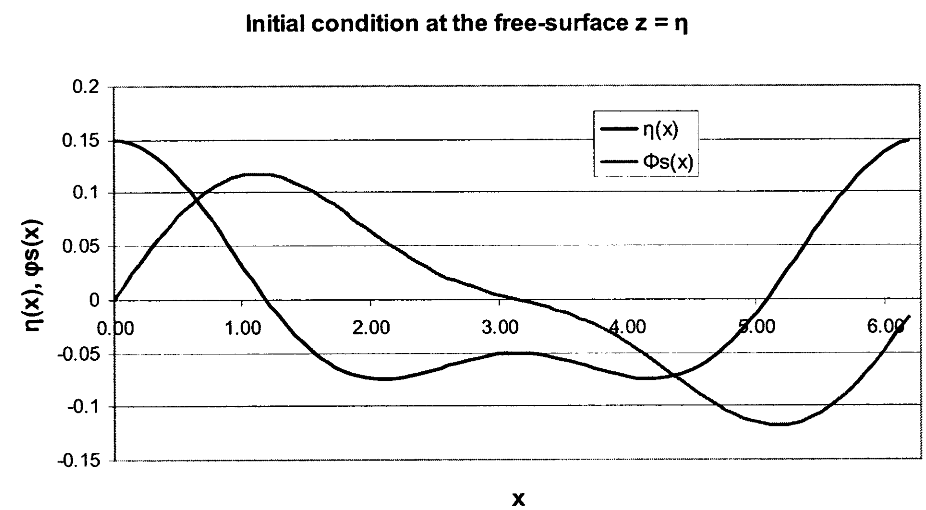

Figure D2 Initial condition of the free-surface elevation and velocity potential for case A1

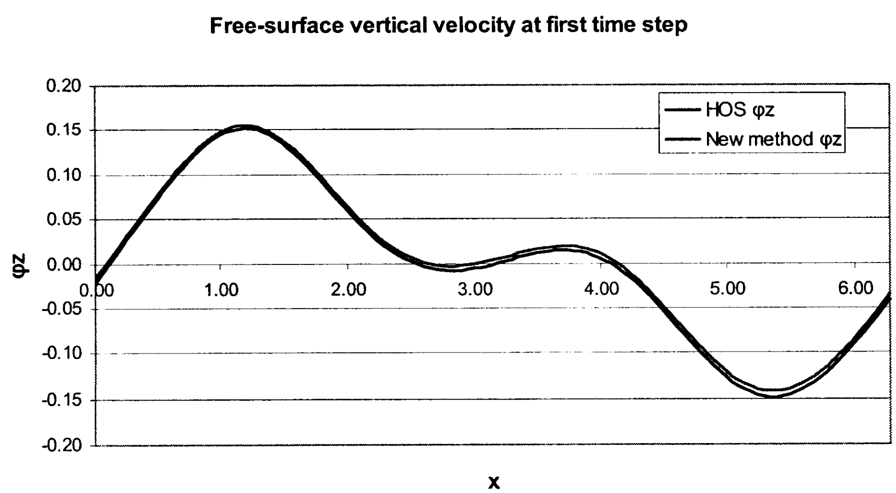

Figure D3 Free-surface vertical velocity φz at $t = t_1$ for case A1

Case A2

Wave characteristics:

- Long wave $A_L = 0.1$, $k_L = 1$
- Short wave $A_S = 0.01$, $k_S = 10$

Study Parameters:

- Steepness $\varepsilon = A_S k_S = A_L k_L = 0.1$
- Length scale $\delta = \lambda_S / \lambda_L = 0.1$

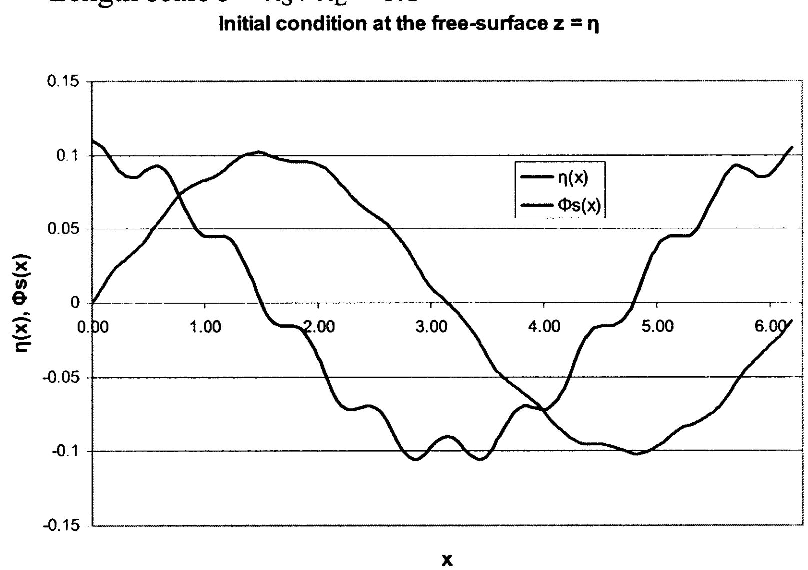

Figure D4 Initial condition of the free-surface elevation and velocity potential for case A2

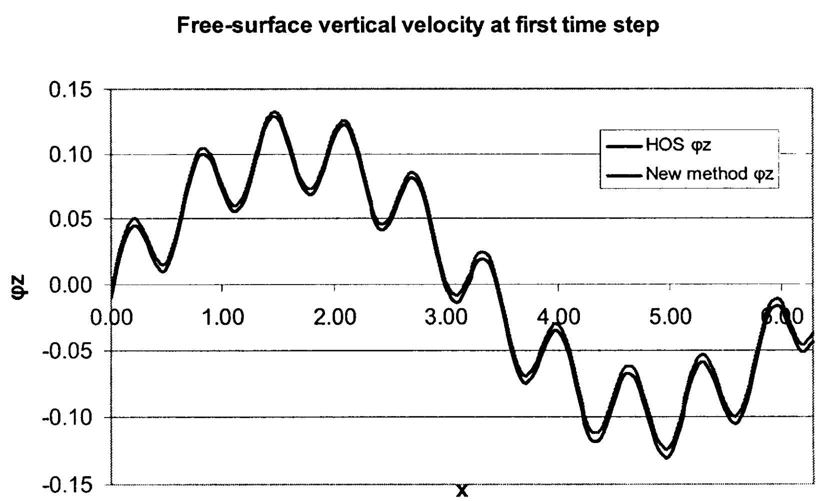

Figure D5 Free-surface vertical velocity φz at $t = t_1$ for case A2

Case A3

Wave characteristics:

- Long wave $A_L = 0.1$, $k_L = 1$
- Short wave $A_S = 0.001$, $k_S = 100$

Study Parameters:

- Steepness $\varepsilon = A_S k_S = A_L k_L = 0.1$
- Length scale $\delta = \lambda_S / \lambda_L = 0.01$

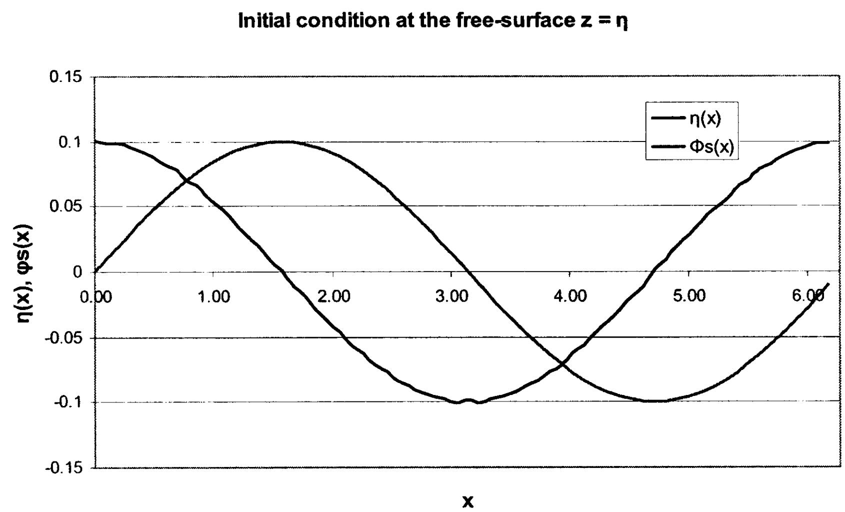

Figure D6 Initial conditions of the free-surface elevation and velocity potential for case A3

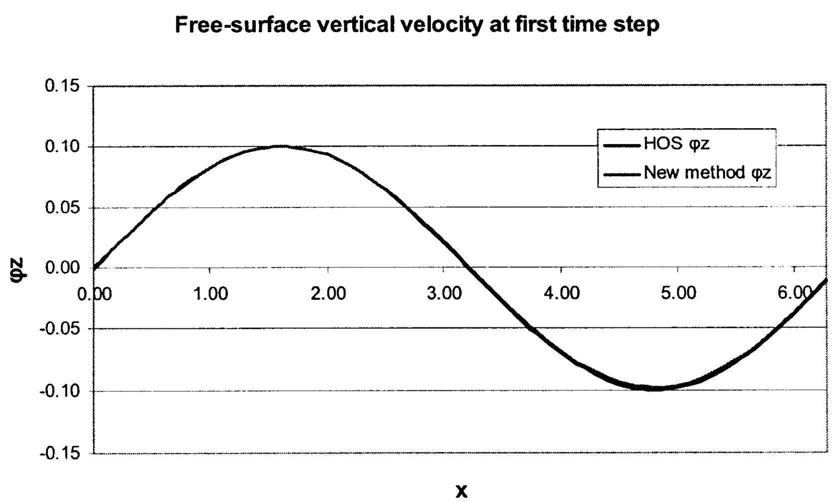

Figure D7 Free-surface vertical velocity φz at $t = t_1$ for case A3

Case A4

Wave characteristics:

- Long Wave $A_L = 0.1$, $k_L = 1$
- Short wave $A_S = 0$

Study Parameters:

- Steepness $\varepsilon = A_S k_S = A_L k_L = 0.1$
- Length scale $\delta = \lambda_S / \lambda_L = 0$

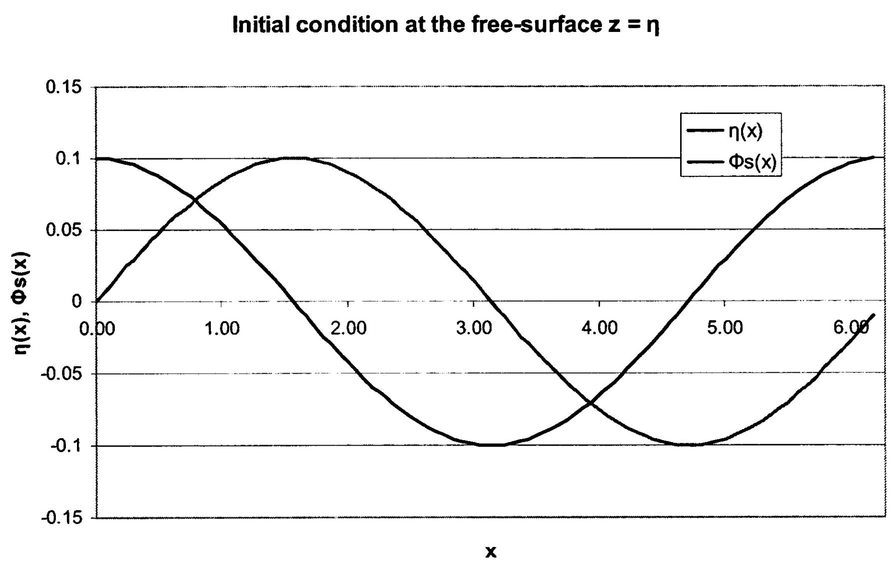

Figure D8 Initial condition of the free-surface elevation and velocity potential for case A4

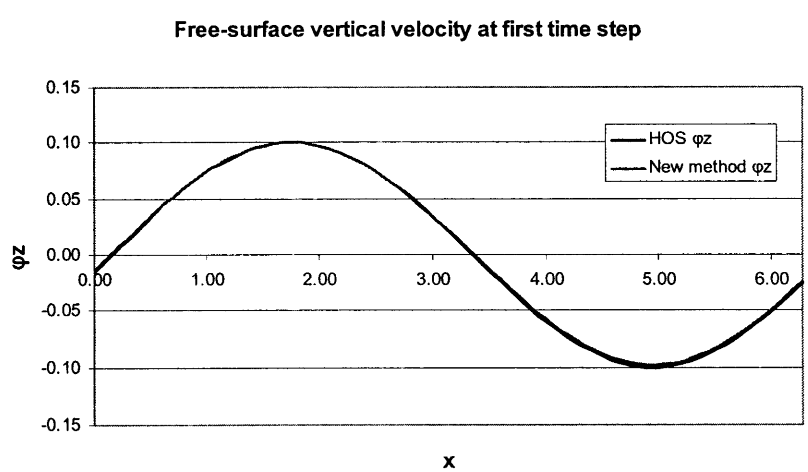

Figure D9 Free-surface vertical velocity φz at $t = t_1$ for case A4

Case B1

Wave characteristics:

- Long wave $A_L = 0.2$, $k_L = 1$
- Short wave $A_S = 0.1$, $k_S = 2$

Study Parameters:

- Steepness $\varepsilon = A_S k_S = A_L k_L = 0.2$
- Length scale $\delta = \lambda_S / \lambda_L = 0.5$

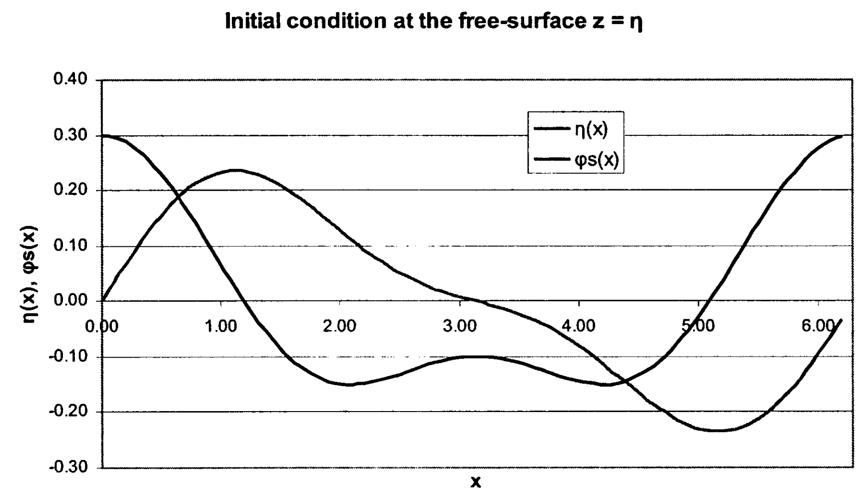

Figure D10 Initial condition of the free-surface elevation and velocity potential for case B1

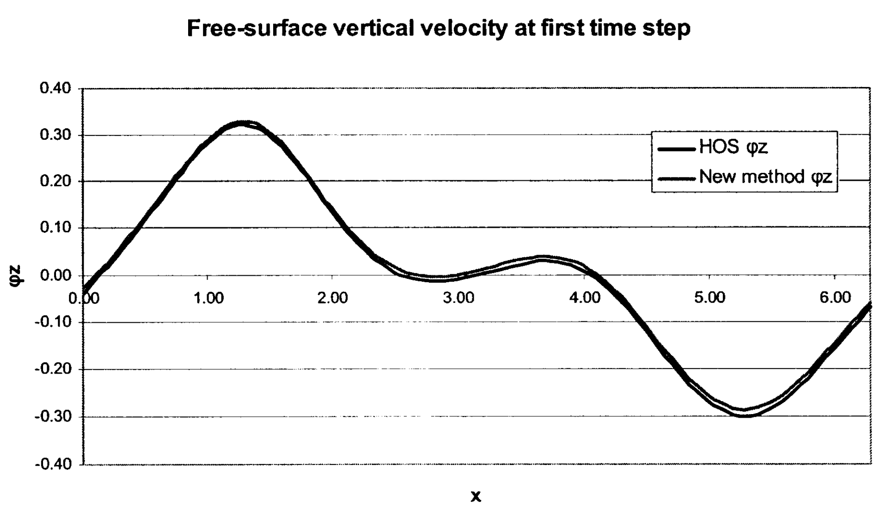

Figure D11 Free-surface vertical velocity φz at $t = t_1$ for case B1

Case B2

Wave characteristics:

- Long wave $A_L = 0.2$, $k_L = 1$
- Short wave $A_S = 0.02$, $k_S = 10$

Study Parameters:

- Steepness $\varepsilon = A_S k_S = A_L k_L = 0.2$
- Length scale $\delta = \lambda_S / \lambda_L = 0.1$

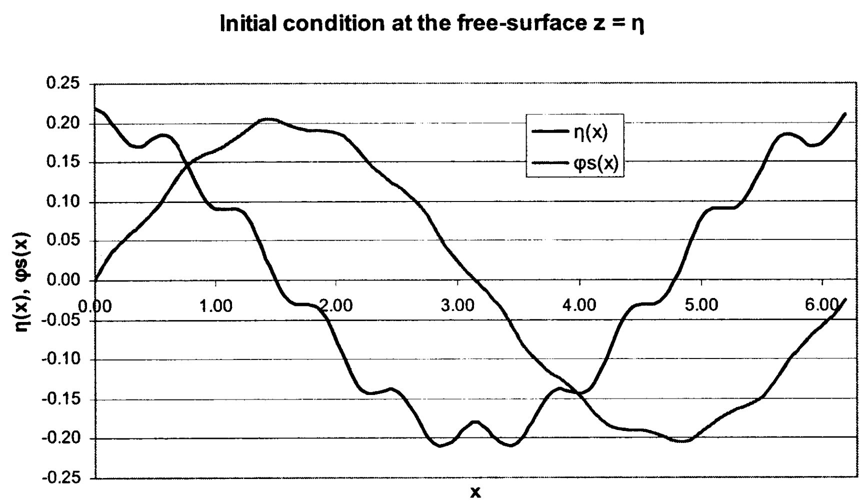

Figure D12 Initial condition of the free-surface elevation and velocity potential for case B2

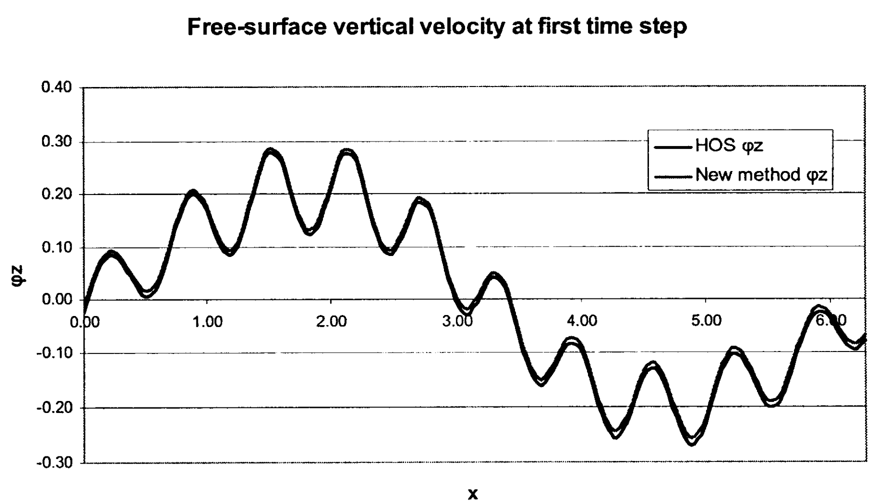

Figure D13 Free-surface vertical velocity φz at $t = t_1$ for case B2

Case B3

Wave characteristics:

- Long wave $A_L = 0.2$, $k_L = 1$
- Short wave $A_S = 0.002$, $k_S = 100$

Study Parameters:

- Steepness $\varepsilon = A_S k_S = A_L k_L = 0.2$
- Length scale $\delta = \lambda_S / \lambda_L = 0.01$

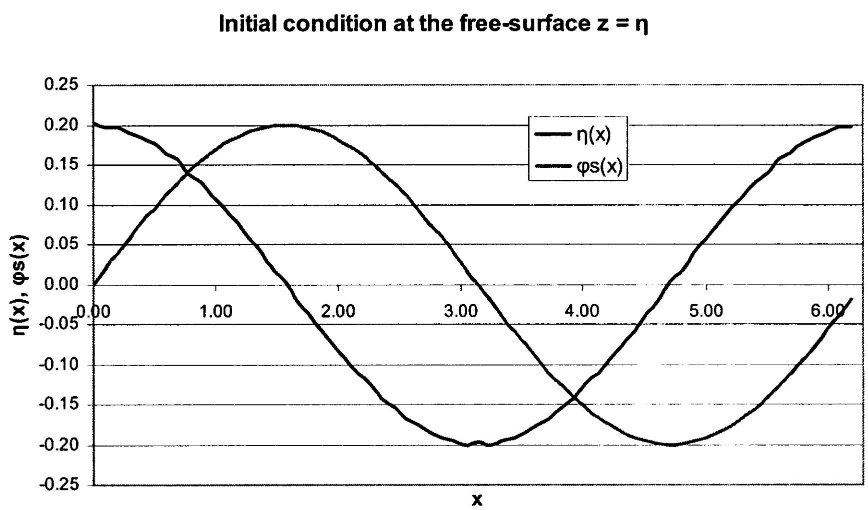

Figure D14 Initial condition of the free-surface elevation and velocity potential for case B3

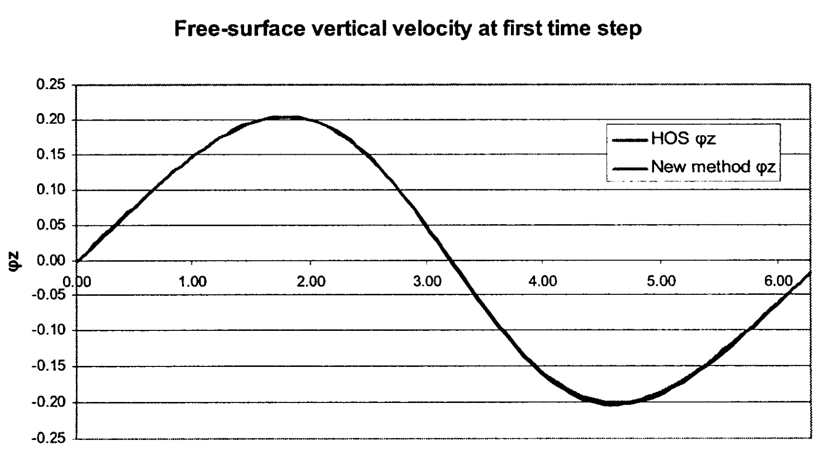

Figure D15 Free-surface vertical velocity φz at $t = t_1$ for case B3

Case B4

Wave characteristics:

- Long Wave $A_L = 0.2$, $k_L = 1$
- Short wave $A_S = 0$

Study Parameters:

- Steepness $\varepsilon = A_S k_S = A_L k_L = 0.2$
- Length scale $\delta = \lambda_S / \lambda_L = 0$

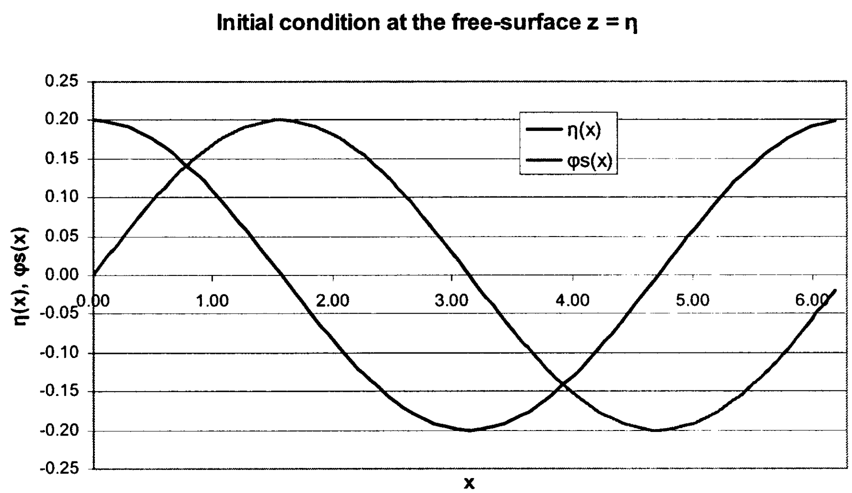

Figure D16 Initial condition of the free-surface elevation and velocity potential for case B4

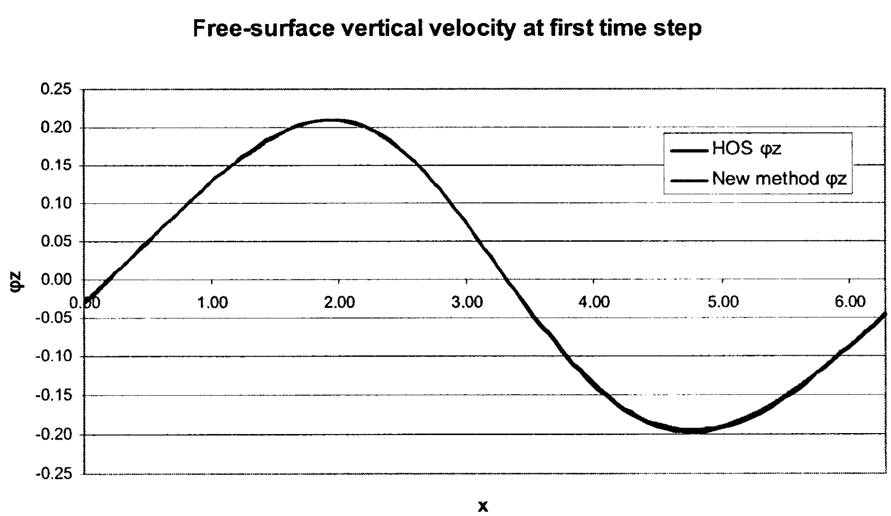

Figure D17 Free-surface vertical velocity φz at $t = t_1$ for case B4

Case C1

Wave characteristics:

- Long wave $A_L = 0.3$, $k_L = 1$
- Short wave $A_S = 0.15$, $k_S = 2$

Study Parameters:

- Steepness $\varepsilon = A_S k_S = A_L k_L = 0.3$
- Length scale $\delta = \lambda_S / \lambda_L = 0.5$

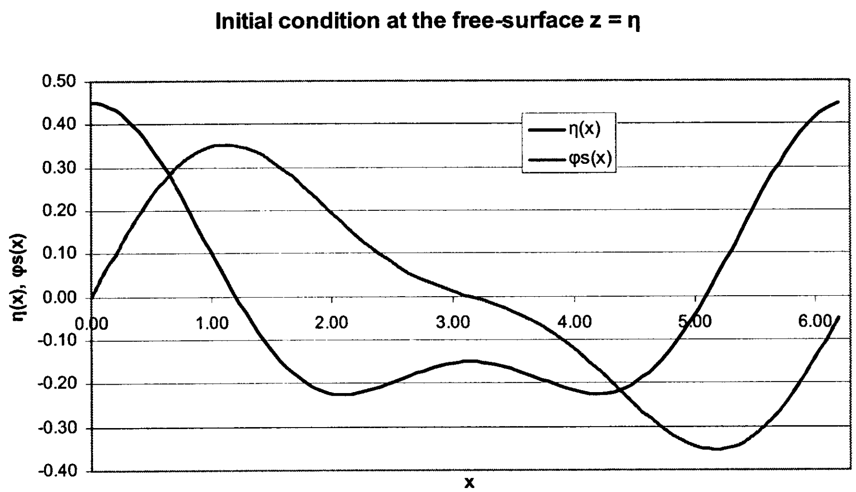

Figure D18 Initial condition of the free-surface elevation and velocity potential for case C1

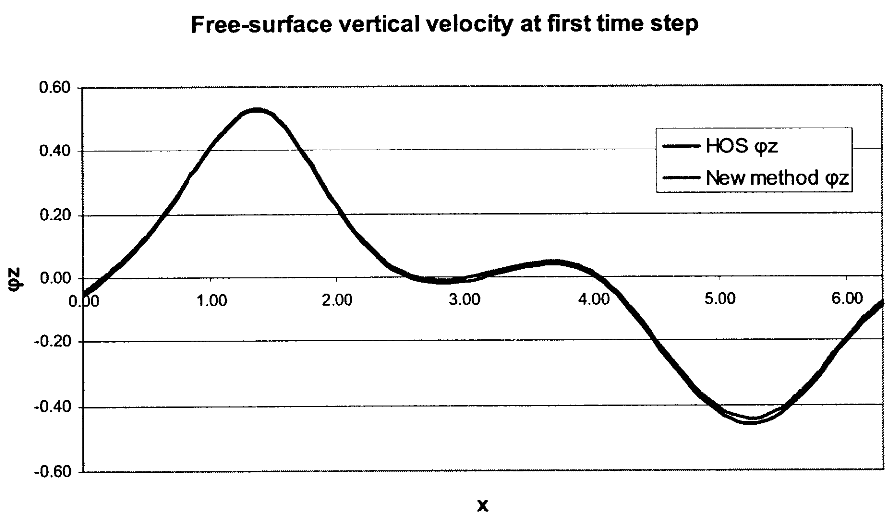

Figure D19 Free-surface vertical velocity φz at $t = t_1$ for case C1

Case C2

Wave characteristics:

- Long wave $A_L = 0.3$, $k_L = 1$
- Short wave $A_S = 0.03$, $k_S = 10$

Study Parameters:

- Steepness $\varepsilon = A_S k_S = A_L k_L = 0.3$
- Length scale $\delta = \lambda_S / \lambda_L = 0.1$

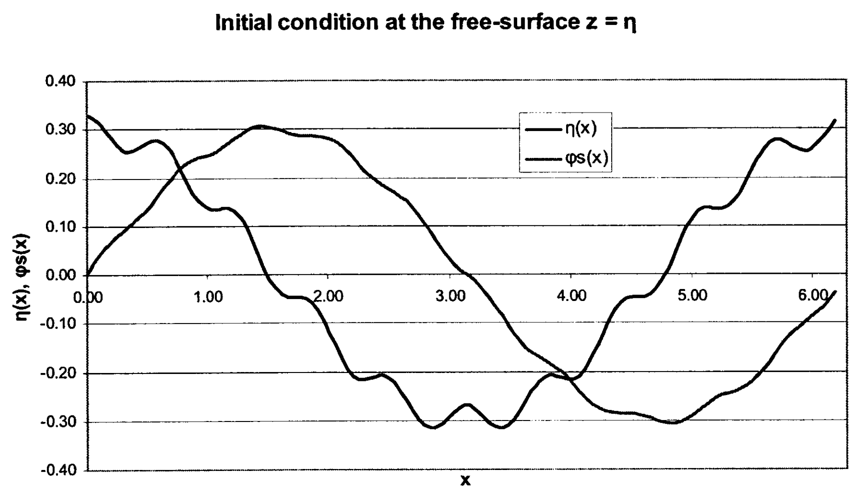

Figure D20 Initial condition of the free-surface elevation and velocity potential for case C2

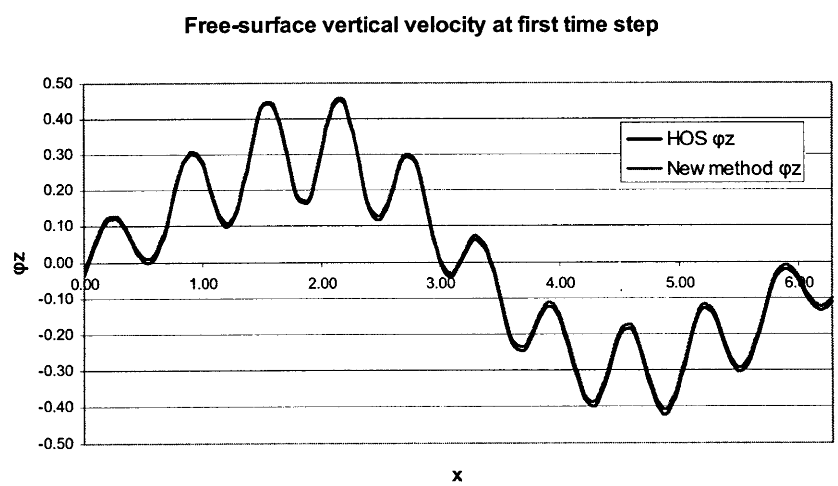

Figure D21 Free-surface vertical velocity φz at $t = t_1$ for case C2

Case C3

Wave characteristics:

- Long wave $A_L = 0.3$, $k_L = 1$
- Short wave $A_S = 0.003$, $k_S = 100$

Study Parameters:

- Steepness $\varepsilon = A_S k_S = A_L k_L = 0.3$
- Length scale $\delta = \lambda_S / \lambda_L = 0.01$

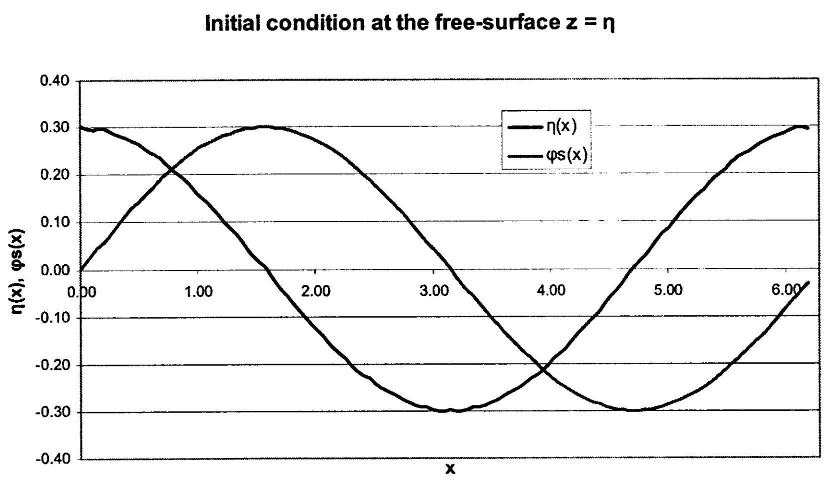

Figure D22 Initial condition of the free-surface elevation and velocity potential for case C3

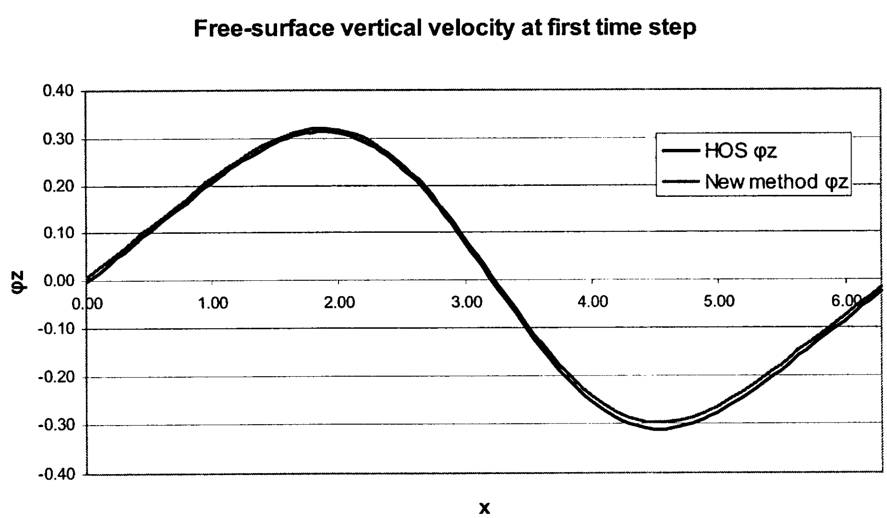

Figure D23 Free-surface vertical velocity φz at t = t_1 for case C3

Case C4

Wave characteristics:

- Long Wave $A_L = 0.3$, $k_L = 1$
- Short wave $A_S = 0$

Study Parameters:

- Steepness $\varepsilon = A_S k_S = A_L k_L = 0.3$
- Length scale $\delta = \lambda_S / \lambda_L = 0$

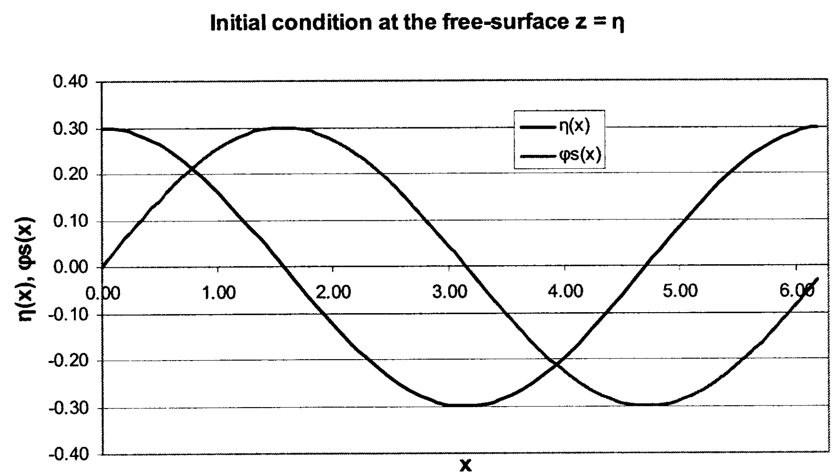

Figure D24 Initial condition of the free-surface elevation and velocity potential for case C4

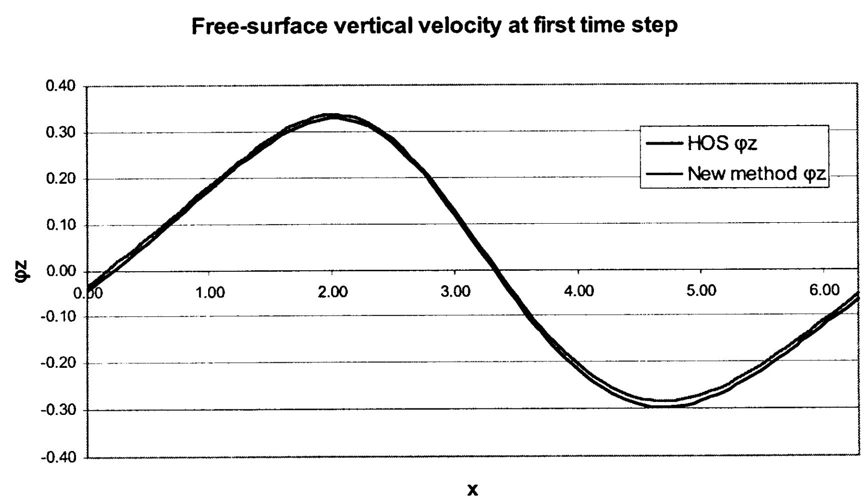

Figure D25 Free-surface vertical velocity φz at $t = t_1$ for case C4

References

Benjamin, T. B. & Feir, J. E. (1967) The disintegration of wave trains on deep water. Part 1. Theory, J. Fluid Mech. 27, 417-430.

Benney, D. J. & Newell, A. C. (1967) The propagation of nonlinear wave envelopes. J. Math. Phys. 46, 133-139.

Boyd, J. P., Chebyshev and Fourier Spectral Methods, Second Edition, DOVER Publications, Inc. (2000).

Bretherton, F. P. & Garrett, C. J. R. (1968) Wavetrains in inhomogeneous moving media. Proc. R. Soc. Lond. A. 302, 529-554.

Bruecknert, K. A.& West B. J. (1988) Vindication of mode-coupled descriptions of multiple-scale water wave .elds. J. Fluid Mech. 196, 585-592.

Chu, V. H. & Mei C. C. (1971) Nonlinear evolution of Stokes waves in deep water. J. Fluid Mech. 47, 337-351.

Dommermuth, D. G. & Yue, K. P. D. (1987). A high-order spectral method for the study of nonlinear gravity waves. J. Fluid Mech. 184, 267-288.

Fornberg, B., A Practical Guide to Pseudospectral Methods, Cambridge Monographs on Applied and Computational Mathematics, Cambridge University Press (1998).

Hasimoto, H & Ono, H. (1972) Nonlinear modulation of gravity waves. J. Phys. Soc. Japan. 33, 805-811.

Lighthill, M. S. (1965) Contributions to the theory of waves in nonlinear dispersive systems. J. Inst. Maths. Appls. 1, 293-306.

Longuet.Higgins, M. S. & Steward, R. W. (1960) Changes in the form of short gravity waves on long waves and tidal currents. J. Fluid Mech. 8, 565-583.

Longuet.Higgins, M. S. & Steward, R. W., (1960) The changes in amplitude of short gravity waves on steady, non-uniform currents. J. Fluid Mech. 10, 529-549, 40

Mei, C. C., Theory and applications of ocean surface waves Part 1: Linear Aspects, Singapore, Hackensack, NJ : World Scientific, c2005.

Mei, C. C., Theory and applications of ocean surface waves Part 1: Nonlinear Aspects, Singapore, Hackensack, NJ : World Scientific, c2005.

Milder, M. D., (1990) The effects of truncation on surface-wave Hamiltonians. J. Fluid Mech. 216, 249-262.

Nicholls, D. P. & Reitich, F (2004) Shape deformations in rough-surface scattering: cancellations, conditioning, and convergence J. Opt. Soc. Am. A Vol. 21, 4, 590-605.

Nicholls, D. P. & Reitich, F (2004) Shape deformations in rough-surface scattering: improved algorithms J. Opt. Soc. Am. A Vol. 21, 4, 606-621.

Nicholls, D. P. & Reitich, F (2005) On analyticity of travelling water waves Proc. R. Soc. 461, 1283-1309, 41.

Nicholls, D. P. & Reitich, F (2006) Stable, high order computation of travelling water waves in three dimensions. Eur. J. Mech. Fluids. 25, 406-424.

Phillips., O. M. (1981) The dispersion of short wavelets in the presence of a dominant long wave. J. Fluid Mech. 107, 465-485.

Phillips., O. M. (1984) On the response of the short ocean wave components at a fixed
wavenumber to ocean current variations. J. Phys. Oceanogr. 14, 1425-1433.

Schwartz, L. W. (1974). Computer extenstion and analytic continuation of Stokes' expansion for gravity waves. J. Fluid Mech. 62, 553-578.

Trefethen, L. N., Spectral Methods in Matlab, SIAM Philadelphia, PA (2000).

West, Bruce J.(1981) On the simpler aspects of nonlinear fluctuating deep water gravity waves (Weak interaction theory) Berlin, New York, Springer-Verlag.

West, B J. Brueckner, K A. & Janda, R. S. (1987) A new numerical method for surface hydrodynamics. J. Geoph. Res. 92, 11803-11824.

Whitham, G. B. (1965) A general approach to linear and nonlinear dispersive waves ising a Lagrangian. J. Fluid Mech. 22, 273-283.

Whitham, G. B. (1974). Linear and nonlinear waves. Wiley, New York.

Zakharov, V. E. (1968). Stability of periodic waves of finite amplitude on the surface of a deep fluid. Zhurnal Prildadnoi Mekhaniki i Tekhnicheskoi Fiziki, Vol. 9, No. 2, pp. 86-94

Zhang, J & Melville, W. K. (1990). Evolution of weakly nonlinear short waves riding on long gravity wabes. J. Fluid Mech. 214, 321-346.